***Graphical Abstract - Synopsis (for review)**

Click here to download Graphical Abstract - Synopsis (for review): TOC.docx

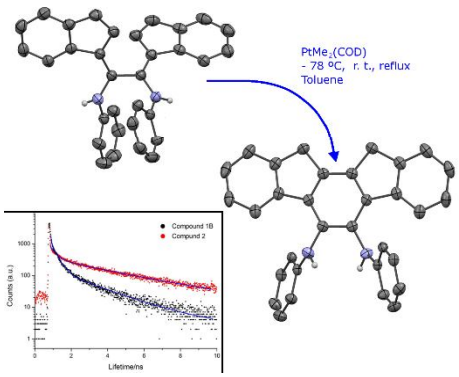

Reaction between lithium indenyl and a chlorine substituted alpha diimine of the form $[\{Cl(NPh)_2\}C)]_2$ yielded the corresponding NH rearranged derivative, rather than the symmetrical α-diimine. The reactivity of **1** towards simple inorganic and organometallic transition metals precursors based on the MX_2 synthons, was investigated. In the case of the reaction with $[PtMe_2(COD)]$ the coupling reaction between the indenyl groups incorporated at the C-C ligand backbone was observed.

Investigations into the reactivity of lithium indenyl with alpha diimines with chlorinated backbones and formation of related functional ligands and metal complexes[1]

Chi-Tien Chen,*[a,b] Mark E. Fischer,[b] Caroline Windsor, [b] Ino C. Vei,[b] David G. Calatayud,[c,d] Malcolm L. H. Green[b] and Sofia I. Pascu*[b,c]

Reaction between lithium indenyl and a chlorine substituted alpha diimine of the form $[\{Cl(NPh)_2\}C)]_2$ unexpectedly yielded the corresponding NH rearranged derivative $[PhN(H)C(C_9H_6)]_2$ (**1**) rather than the predicted symmetrical α-diimine. This compound **1** was characterised by ^1H NMR, $^{13}C\{^1H\}$ and mass spectrometry, and additionally by X-ray diffraction. It was found that **1** was the first indene-substituted and symmetric secondary amine which was also highly fluorescent in DMSO. The reactivity of **1** towards simple inorganic and organometallic transition metals precursors based on the MX_2 fragments, where M = Group 10 metals and X = halides or methyl groups, has been investigated. Surprisingly, the reaction with $[PtMe_2(COD)]$ led to the coupling reaction between the indenyl groups incorporated at the C-C ligand backbone and a new ligand (**2**) was discovered, in an attempt to synthesise the metal-linked diamine. Single crystal X-ray diffraction studies confirm this compound **2** to feature coupled indenyl residues and delocalised C-C bonds in the solid state. Structural authentication by X-ray crystallography showed compound **2** to be a very rare example of flat and extended aromatic organic molecule and mass spectrometry, IR and NMR spectroscopy were carried out to gain further insight into the solid state and solution phase structures. Further experiments to synthesise analogues of $[PhN(H)C(Ind)]_2$ aiming to shift a likely equilibrium in favour the imine tautomer, by introducing bulky *ortho* substituents onto the benzene ring (R = Me, iPr) showed the presence of the imine tautomer to be increasingly favoured in ^1H NMR spectra, with an increase in the steric bulk of the *ortho* substituents. However, the enamine tautomer is still observed to a minor extent even with isopropyl substituents and yields of these desired compounds were low on steric grounds.

INTRODUCTION

The discovery of the α-diimines led to the preparation of the Brookhart-type Group 10 catalysts, which constituted a paradigm shift in transition metals catalysis in the last decade of the 20th century [1-7]. Bis(imidoyl)chloride, a versatile ligand incorporating both diimine and dichloride functionalities can be used as a starting material in the synthesis of diimine [8], heterocyclic [9, 10] or oxalamidine [11, 12] ligands when reacted with the suitable alkyl group, dianions or amines [13]. The steric and electronic effects of these versatile ligands are known to be programmable through the variations of the substituents on the nitrogen atoms [11] and to the groups attached to the carbon atoms. The diimine-containing ligands have attracted interest, mainly driven by the discovery that the late transition metal diimine complexes display efficient activity in catalysing the olefin polymerisation reaction [7, 14-24]. Furthermore, the well-known metallocene compounds also display excellent catalytic ability in olefin polymerisation reactions [25]. Therefore, studies to prepare ligands containing the two types of donor groups have been explored [26].

Tuning the electronic and structural properties of the ligand by changing its donor functionalities (in type and / or number), bite angle, bulkiness and chirality, has marked effects on transition metal catalysis [2, 3, 27, 28]. We describe here the synthesis and characterisation of a new class of ligands. These were designed such that they may held two pre-catalytic metallic centres in close proximity to the rigid framework reminiscent of an ansa-metallocene-derivatised bulky diimine. Such system might combine the different advantages of catalytic processes within early and late transition metal systems to generate new catalysts for coupling reactions, of interest for both academic and industrial research [29-31].

In spite of some significant advances in the chemistry of transition metals chemistry over the past decade [7, 25, 32-34], including the reports considered advances in ligand design for heterobimetallic chemistry [35-40], the quest for molecules and materials with

[1] Address:
[a] National Chung Hsing University, Department of Chemistry 250, Kuo Kuang Rd., Taichung 402, Taiwan R.O.C.
[b] Inorganic Chemistry Laboratory, South Parks Road, Oxford, OX2 6TT
[c] Department of Chemistry, University of Bath, Claverton Down, BA2 7AY, E-mail: s.pascu@bath.ac.uk
[d] Department of Electroceramics, Instituto de Ceramica y Vidrio CSIC, Kelsen 5, Campus de Cantoblanco, 28049 Madrid, Spain

catalytic properties thus far unexplored is ongoing, leading to new chemistry of relevance to enhancing our understanding of future processes for sustainable chemistry applications.

We describe here the synthesis and characterisation of a new class of mixed ligands based on bis(imidoyl)chloride, and the exploration of their chemistry. Some related design attempts have been made recently involving organic chemistry approaches and led to the synthesis of a couple of examples of fluorescent molecules with antibacterial applications, but no catalytic applications have been pursued thus far [41]. Here we also build upon our earlier forays into establishing the synthetic methodology and delineating the challenges encountered at the synthesis of new organic ligands having the combined the ability of the donor centres to bind to early- or late- transition metals [31-33, 42]. Since late TM-catalysts produce oligomers or highly-branched polyolefins [25] and early metallocenes generate linear (non-branched) polyolefins [43], our ligand system designed as shown in Scheme 1, opens up new prospects for the formation of functional 'polymers of oligomers' with properties as yet unobserved.

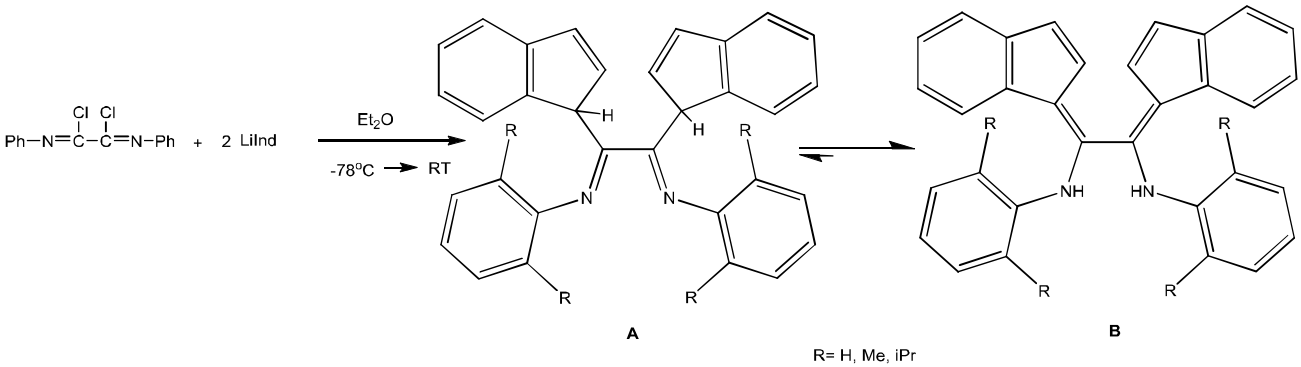

Scheme 1. Preparation of $[2,6\text{-}R_2C_6H_3\text{-}N(H)C(C_9H_6)_2]_2$. Proposed equilibrium between the diimine and dienamine tautomers of $[ArNC(Ind)]_2$ for compound **1** (R=H).

RESULTS AND DISCUSSIONS

Synthesis and characterisation of the $[C_6H_5NH\text{-}C(C_9H_6)\text{-}C(C_9H_6)\text{-}NHC_6H_5]$, 1

Preparation of lithium indenyl from indene and *n*BuLi followed an adaptation of the literature methods [9] leading to a highly air- and moisture-sensitive off-white powder, which was immediately used in the next reaction step. As such, two equivalents of lithium indenyl in diethyl ether cooled to -78°C were added dropwise to a suspension of one equivalent of $[PhN=C(Cl)]_2$ in diethyl ether at -78°C. After 18 hours, while allowing the reaction mixture to reach room temperature, the volatiles were removed and the bright-red precipitate extracted into CH_2Cl_2 giving rise to a bright-red powder. This was washed in diethyl ether at -78°C to give the desired product compound **1** which was deemed analytically pure by elemental analysis and NMR spectroscopy. Interestingly, the compound was identified by ^1H and $^{13}C\{^1H\}$ NMR and X-ray crystallography as an α-dienamine of the form **B** (Scheme 1) rather than the expected α-diimine compound. Similar procedures were adapted and employed for the analogous reactions between indenyl lithium and related chlorine substituted alpha diimines of the form $[PhN=C(Cl)]_2$, where R = Me and ^{i}Pr, however no pure derivative of either type A or B alone could be isolated alone thus far when such bulky substituents were employed. Instead, for R = Me or iPr, VT ^1H NMR experiments in d-toluene or CD_2Cl_2 showed that, unlike the case when R = Ph, an inseparable mixture of the isomers **A** and **B**, as well as the related, mixed, imine-enamine derivative (denoted **C**) were thus far identified as the species present simultaneously in solution for R = Me and ^{i}Pr (*vide infra*).

To characterise compound **1**, a series of spectroscopic methods were employed and the findings are discussed below. The assignments, made by determination of the coupling constants and of the ^1H-^1H COSY NMR spectra point out that, instead of the target compound, the α-diimine form denoted **1A** for the $[PhNC(C_9H_7)]_2$, the α-dienamine tautomer of the desired product Scheme **1B** was obtained.

For R=H (compound **1**), the ^1H NMR (C_6D_6) spectrum of the emerging product exhibits a singlet at δ 6.06, assignable to the protons resonances localised at the two nitrogen centres as it does not couple into any other resonance by the ^1H-^1H COSY spectroscopy experiment. The assignment of this resonance as an indenyl C-bound proton would be inconsistent with the diimine structure of the isomer **A** given in Scheme 1 (**A**) which would be expected to exhibit resonances with vicinal coupling. All other proton resonances are assignable in a manner consistent with the rest of the α-dienamine structure.

Variable temperature ^{1}H NMR experiments in either d_8-toluene, THF or CD_2Cl_2 showed some slight broadening of the resonances, but the isolation of the isomer **1A** from the mixture could not be demonstrated, and it is currently believed that the equilibrium was shifted firmly towards the formation of **1B** during the reaction process.

The $^{13}C\{^{1}H\}$ NMR (C_6D_6) spectrum showed 16 signals, in the range δ 144.2 to 118 ppm, consistent with the number of non-equivalent carbon atoms in the compound. All carbons are sp^2 hybridised and either secondary or tertiary and thus fall in a rather narrow chemical shift range. The infrared spectroscopy of the product recorded in the solid state further supports the hypothesis that the hydrogens are more likely bound to the nitrogen atoms rather than the indenyl groups. Thus, a sharp, rather intense single peak is observed at 3390 cm^{-1} indicative of an N-H stretch, as well as some broader signals in the 1588 cm^{-1} region of the spectrum, assignable to a C=N or electron-delocalized N(H)C group.

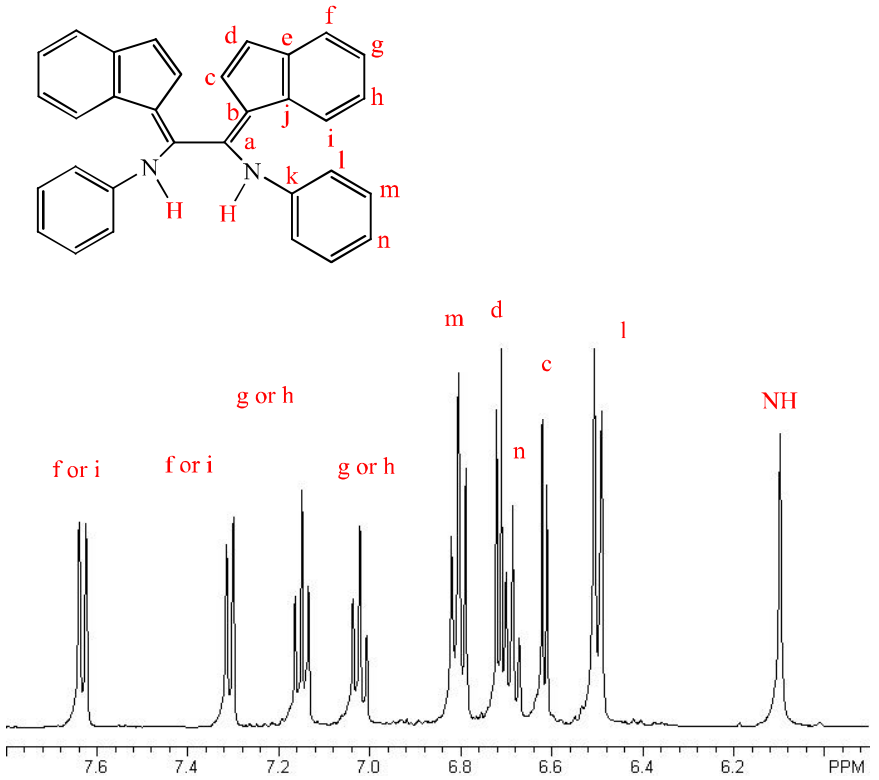

Figure 1 (a) ^{1}H NMR in C_6D_6 (500 MHz) with assignments emerging from ^{1}H-^{1}H COSY and HMBC experiments showing the resonance assignments for compound **1**, as isomer **B**. Detailed assignments for sample in CD_2Cl_2 are also given in Experimental section.

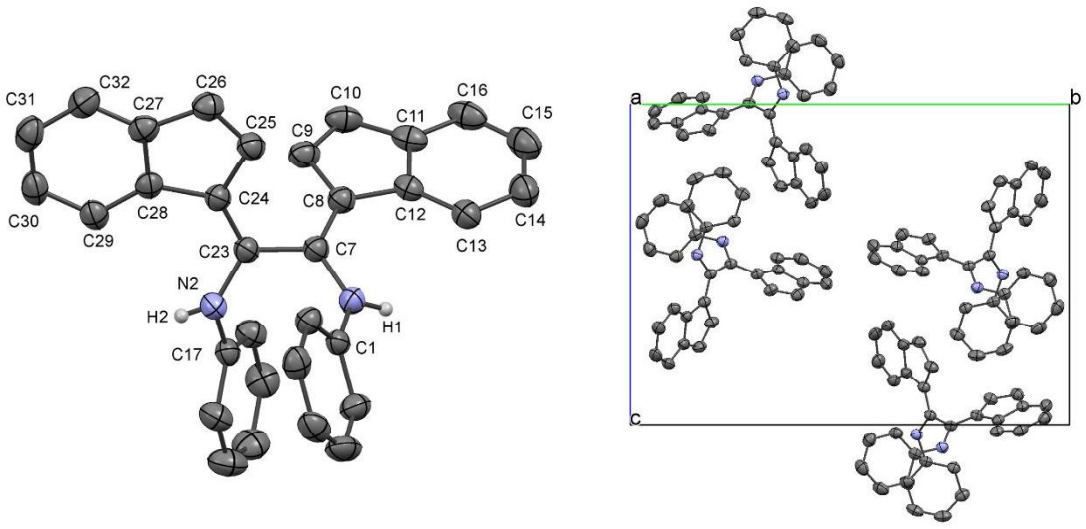

Figure 2. The molecular structure of [C_6H_5NH-$C(C_9H_6)$-$C(C_9H_6)$-NHC_6H_5] and crystal packing (**1B**). Hydrogen atoms on the indenyl and on the phenyl groups are omitted for clarity. The H attached at the N(1) and N(2) were localised in Fourier maps. Ellipsoids at 50% of probability.

Dark-red crystals of compound **1B** suitable for X-ray refinement were grown from a concentrated diethyl ether solution layered with pentane at -25 ºC. A crystal of dimensions 0.30 x 0.40 x 0.80 mm was chosen under an inert atmosphere, covered with perfluoropolyether oil, and mounted on the end of glass fibre. The data were collected at 293(2) K and indexed on a monoclinic cell, consistent with the *P21/c* space group. The molecular structure is shown in Figure 2 and selected bond distances and angles are listed in Table 1. Full bond distances and angles are listed in Table S1, ESI. The molecular structure is symmetric and confirms that the hydrogen atoms are not placed at the expected carbon centres, but rather attached to the nitrogen atoms which are in a secondary amine form, and overall the compound **1B** can be regarded as a dienamine instead of the expected diimine compound. It is likely that the H's migrated via a 1,3-shift from the carbon atoms in the indenyl groups during the synthesis. The bond lengths N(1)-C(7) and N(2)-C(23) are found to be of distances between the typical values for covalent single C-N and double C=N (1.47 Å and 1.27 Å respectively (1.3759(15) Å and 1.3791(15) Å respectively) [10]. The bond lengths C(7)-C(8) and C(23)-C(24) are closer to the distances found in typical double C=C bonds (1.3725(16) Å and 1.3652(17) Å respectively) than in single C-C bond (ca. 1.54 Å). The bond lengths of C(9)-C(10), 1.349(2) Å, and C(25)-C(26), 1.3474(19) Å, are also closer to double C=C bonds than the rest of the carbon-carbon bonds of the indenyl groups. As expected, the rest of the carbon-carbon distances in the six-carbon ring of the indenyl groups, 1.386(2) to 1.4208(17) Å are having lengths which place them between single bond and double bond and suggest that there is a strong delocalisation over the relevant six carbon atoms of this functionality. The bond angles around C(7), 117.14(10) to 122.26(11)º and C(23), 117.35(10) to 121.66(11)º all reflect the sp^2 character of the bridged carbons.

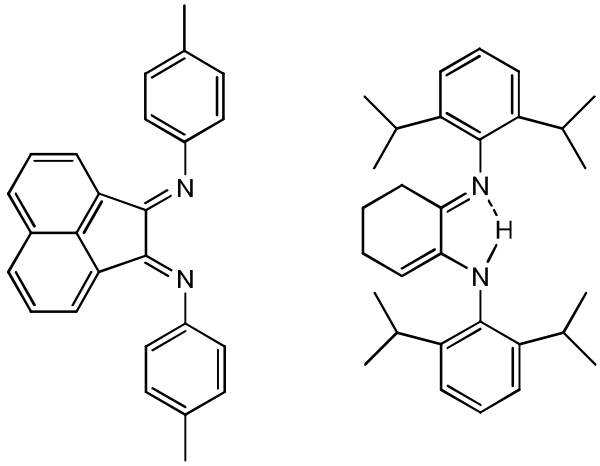

*p*Tol-BIAN [C_6H_3(i-Pr)$_2$]$_2$-AIC

Figure 3. The known, related, ligands *p*Tol-BIAN (diamine) [11] and [C_6H_3(i-Pr)$_2$]$_2$-AIC] [12] showing a mixed imine-enamine form.

These distances can be compared with the diimine compound *p*Tol-BIAN, was fully characterised by Elsevier *et al.* [11]. The α-diimine structure has bond lengths of C(7)-N(1) and C(23)-N(2) of 1.267 Å, typical of C=N bonds, and bond lengths C(1)-C(21) and C(2)-C(41) are 1.480 Å, more typical of C-C bonds. These contrast largely with the bond lengths found in compound **1B**, [$PhN(H)C(C_9H_6)$]$_2$. The bond angles C(1)-N(1)-C(7) and N(1)-C(7)-C(23) of 121.7º and 120.4º, respectively, show deviation away from the equivalent [$PhN(H)C(C_9H_6)$]$_2$ values. Thus this comparison with a typical alpha-diimine further confirms the α-dienamine structure of the ligand. The formation of an α-dienamine ligand rather than of an α-diimine was therefore somewhat unexpected. However, "migration" of protons from the carbon to the nitrogen in such compounds has been reported previously [11, 12]. For example, the rigid compound, [{C_6H_3(i-Pr)$_2$}$_2$-AIC] (Figure 3), was characterised spectroscopically not as the α-diimine but rather as the imine/enamine tautomer [12]. It is thought that the enhanced stability of this form is due to the greater stability of the endocyclic double bond and the formation of an intramolecular hydrogen bridge between the amine and imine N atoms.

In an attempt to shift the reaction shown in Scheme 1 towards the formation of the diimine isomer compound **1A**, the as-formed [$PhN(H)C(Ind)$]$_2$ was treated with [$PtMe_2$(COD)]. This reaction, shown in Scheme 2, was carried out in toluene between -78 ºC and room temperature, as discussed in the Experimental section. ^{1}H NMR spectroscopy of the reaction mixture indicated that no reaction had occurred. The reaction mixture was therefore kept under reflux for one hour, yielding an orange-brown solid and a grey solid. The grey solid was shown by elemental analysis and NMR spectroscopy to contain mainly platinum and decomposition material. ^{1}H- and ^{13}C{^{1}H} NMR spectroscopies of the orange-brown solid, together with X-ray crystal diffraction determination, showed formation of compound **2** with the formula [$PhN(H)C$]$_2$($C_{18}H_{10}$). The presence of the NH proton is confirmed by a singlet in the ^{1}H NMR spectrum (δ 5.68) which

couples to no other protons by the ^{1}H-^{1}H COSY spectroscopy, whilst the IR spectroscopy was inconclusive, showing broad bands both in the 3500 cm^{-1} as well as in the 1500 cm^{-1} regions.

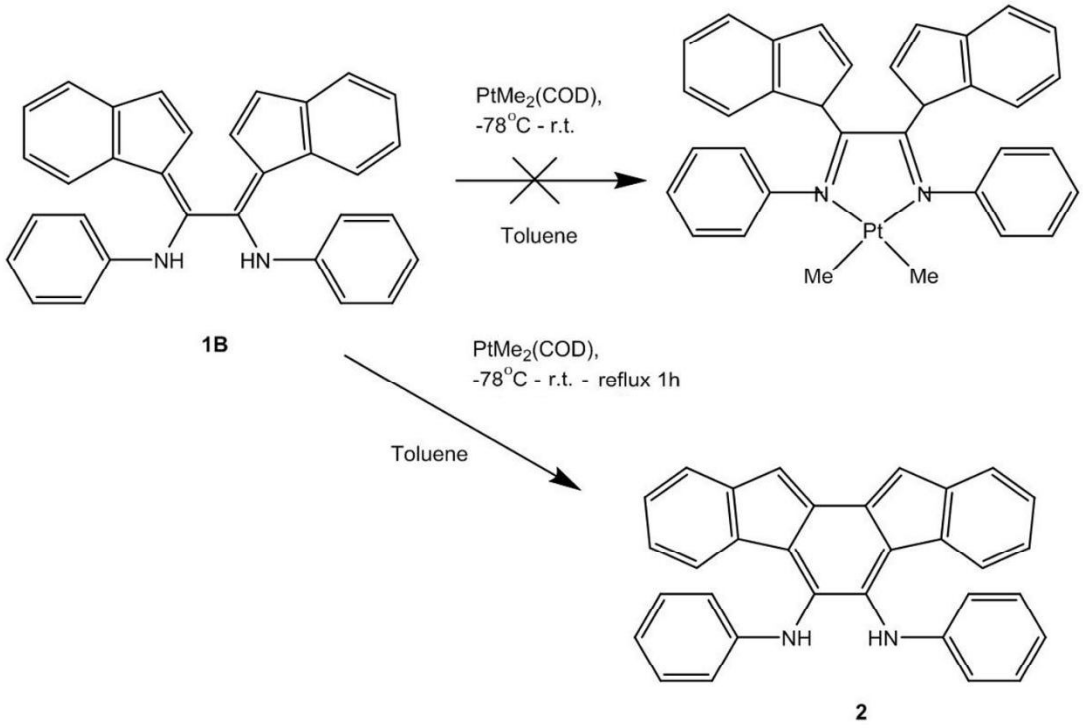

Scheme 2. Reaction between $[PhN(H)C(Ind)]_2$ and $PtMe_2(COD)$

The reflux reaction of $[PhN(H)C(Ind)]_2$ (**1**) in toluene for one hour in the absence of $[Pt(Me)_2(COD)]$ did not result in formation of compound **1**. This suggests that the Pt(II) complex catalyses its formation, leading to Pt(0) and methane elimination. An analogous carbon-carbon coupling has been reported in the state-of-the-art, for a substituted bis-indenyl system, mediated by a Ti(IV)/Ti(III) catalyst system [44].

Figure 4 shows the molecular structure of the compound **2**, viewed in several different selected views to illustrate its planarity. Selected bond lengths and angles emerging from the single crystals X-ray diffraction are given in Table 1. For comparison, the bond lengths and angles of the starting material **1B**, $[PhN(H)C(Ind)]_2$ are also included. The coupled 5-membered rings are co-planar and one NH proton is lying above and the other below their plane. The N(1) - C(7) bond is notably longer than in the starting compound, showing a decrease in the double bond character as formation of the diimine would result in loss of more aromatic stabilisation energy for this compound than the starting compound. Its length is still intermediate in value between the double (typically 1.32 Å) and single (typically 1.51 Å) bond [10] but indicates that this compound is in an enamine form also seen in the reduced C(1)-N(1)-C(7) bond angle of 123.14(16)º, with respect to that of the starting material **1B**, 127.00(10)º.

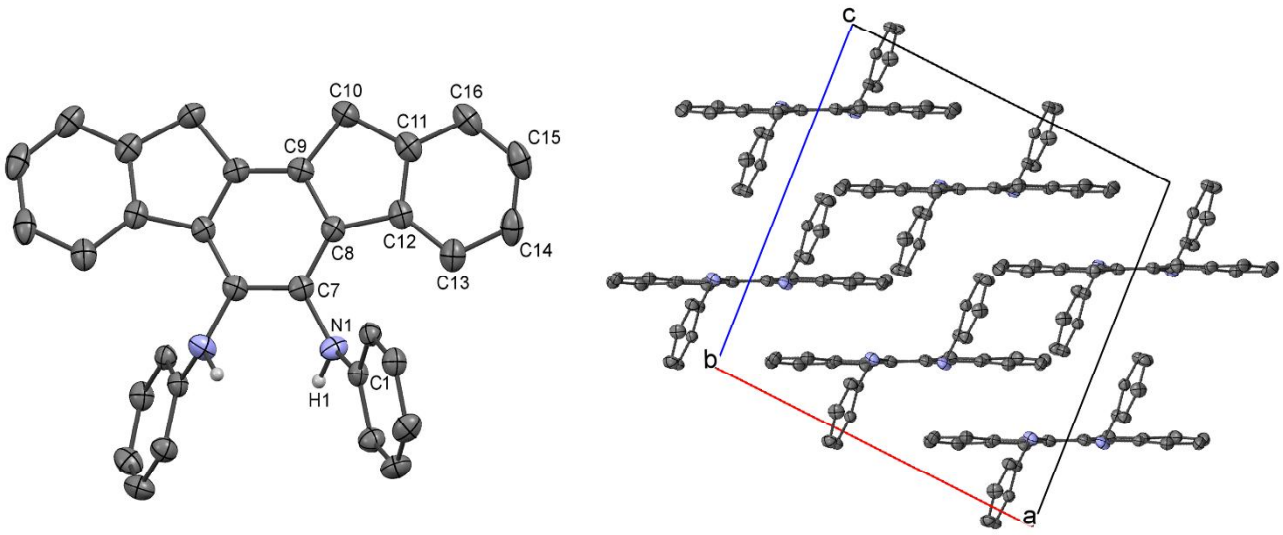

Figure 4. The molecular structure of [PhNH-C(C_9H_6)-C(C_9H_6)-NHPh] (**2**) and crystal packing. Hydrogen atoms on the indenyl and on the phenyl groups are omitted for clarity. The H attached at the N(1) and N(2) were localised in Fourier maps. Ellipsoids at 50% of probability.

Table 1 Selected bond lengths (Å) and angles (º) for **1B** and of the coupled derivative **2**.

	Product Compound 2 [PhN(H)C]$_2$($C_{18}H_{10}$)		**Starting compound 1B [PhN(H)C(Ind)]$_2$**	
Bond Lengths **(Å)**	N(1)-C(1)	1.401(2)	N(1)-C(1)	1.4122(15)
	N(1)-C(7)	1.422(3)	N(1)-C(7)	1.3759(15)
	C(7)-C(8)	1.396(3)	C(7)-C(8)	1.3725(16)
	C(8)-C(9)	1.405(3)	C(8)-C(9)	1.4609(16)
Bond Angles (º)	C(1)-N(1)-C(7)	123.14(16)	C(1)-N(1)-C(7)	127.00(10)
	N(1)-C(7)-C(7)#1	119.38(11)	N(1)-C(7)-C(7)#1	117.14(10)
	N(1)-C(7)-C(8)	121.19(17)	N(1)-C(7)-C(8)	122.26(11)

The C(1)-N(1)-C(7) angle is somewhat greater than the 120º value expected for a trigonal planar geometry. The typical values for C-C single bond of 1.54 Å and C=C double bond of 1.34 Å places the C(7)-C(8) and C(8)-C(9) bonds of intermediate bond length, suggesting delocalisation of electron density across the molecule as would be expected for aromatic compounds. The differences in length compared with the equivalent bonds in the starting material reflect the changes in formal single bond and double bond status. This is seen in the N(1)-C(7)-C(7) #1 and N(1)-C(7)-C(8) bond angles of the two compounds, with a reduced angle for the former and increased angle for the latter parameter in [PhN(H)C(Ind)]$_2$ the result of the greater space required by the formal double bond character of C(7)-C(8) of **1**.

Given that the organic compounds **1B** and **2** both exhibited interesting structures in the solid state, which are incorporating fused aromatic groups, as well as the fact that they are intensely colored (i.e. red and orange/brown, respectively) in solutions, the optical characterization of the compounds was carried out. Two-photon fluorescence emission spectroscopy and lifetime measurements were recorded using time-correlated single photon counting with an excitation wavelength of 910 nm and the emission measured at 360-700 nm (Figure 5). Fluorescence lifetimes of both compounds **1B** and **2** decay as two component systems, with minor components ($\tau 2$) in the order of several nanoseconds (2.0 and 3.5 ns, respectively) and major components ($\tau 1$) in the order of several hundred picoseconds (0.3 and 0.3 ns, respectively, see experimental section)

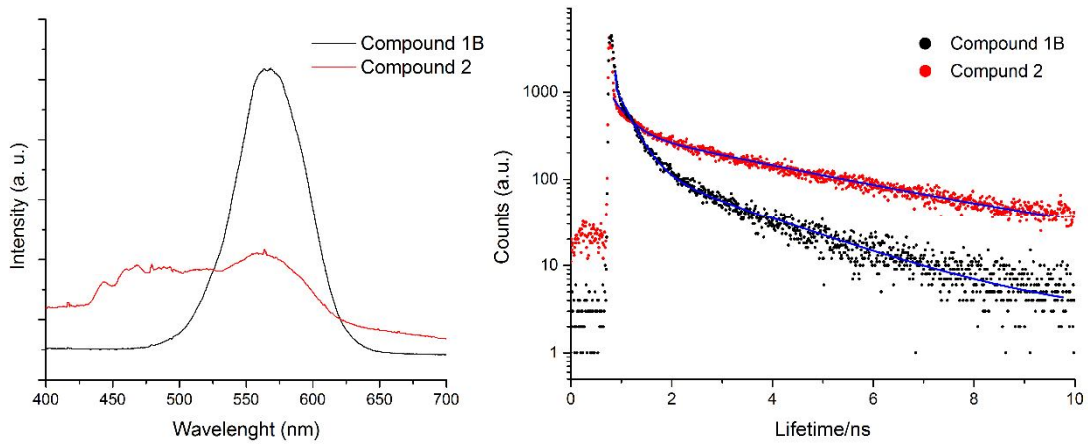

Figure 5. Overlays of (a) Two-photon fluorescence emission spectroscopy and (b) time-correlated single photon counting: fluorescence decay traces and corresponding fitted curves for the lifetime determinations (λ_{ex} = 910 nm, Compounds **1B** and **2**, each in 10 mM conc. in pure DMSO, 5.8 mW).

Reactivity of the ligand [PhN(H)C(C_9H_6)]$_2$ towards MX_2 fragments (M = Group 10 transition metal, X = halides or Me)

Once compound **1** was isolated and characterised, several different for further derivatisation were pursued aiming towards the isolation of new, early-late heterobimetallic metal complexes. Since the labile protons are likely those bound to the nitrogens rather than C-H, there are two possible reactions on deprotonation and subsequent reaction with a Zr(IV) complex precursor such as $Zr(NMe)_4$. It was hypothesised that the negative charge may move to the indenyl ring and therefore allow Zr(IV) co-ordination to form the *ansa*-metallocene. Zirconium(IV), in addition, is known to readily form chelating diamide complexes and the presence of an extended conjugated system may well favour the formation of a α-diamide complex of zirconium. For example, the compound, [1,3-C_3H_6{N(H)$SiMe_3$}$_2$], a known β-diamine, when refluxed in a toluene solution of $Zr(NMe_2)_4$ results in an deamination reaction to afford the β-diamide complex [1,3-C_3H_6{$NSiMe_3$}$_2$$Zr(NMe_2)_2$] [14]. When such synthetic avenues were explored hereby, by reacting compound **1** with $Zr(NMe_2)_4$ in toluene, between -78 ^oC and room temperature over several hours, only formation of a mixture of compounds were obtained, and despite promising analytical data from ^1H NMR the mass spectrometry was difficult to interpret, and further studies are in progress to establish the identity of the emerging compounds.

The treatment of [PhN(H)C(C_9H_6)]$_2$ with Group 10 transition metal precursors, either based on Ni(II) or Pd(II), first were performed as the first functionalisation steps, in an attempt to minimise the likely isomers that emerge from the multiple metal derivatisation of the bis-indenyls observed for Zr(IV) precursors. This approach followed the earlier observations that the known imine/enamine compound [{C_6H_3(i-Pr)$_2$}$_2$-AIC] resulted in the formation of an α-diimine complex on reaction with [$NiBr_2$(DME)] [12]. The ligand [PhN(H)C(C_9H_6)]$_2$ (**1B**) was therefore reacted in the similar way with [$NiBr_2$(DME)] as well as with [$(PhCN)_2PdCl_2$] to give the corresponding [{PhNC(C_9H_7)}$_2$$NiBr_2$] or [{PhNC($C_9H_7$)}$_2$$PdCl_2$] where it was envisaged that the protons bound to the nitrogen atoms would be migrating to the indenyl groups. As such, one equivalent of [$NiBr_2$(DME)] was treated with one equivalent of [PhN(H)C(C_9H_6)]$_2$ in CH_2Cl_2 and the reaction mixture stirred at room temperature for 18 hours. The volatiles were removed and the solid washed in diethyl ether and pentane followed by recrystallisation from CH_2Cl_2 and pentane to give the desired $NiBr_2$-chelated product, denoted **3**, (Scheme 3) upon drying *in vacuo*. The reaction between one equivalent of [$(PhCN)_2PdCl_2$] and one equivalent of [PhN(H)C(C_9H_6)]$_2$ was carried out in the same manner, aiming to obtain the α-diimine form of compound **4**, [{PhNC(C_9H_7)}$_2$$PdCl_2$].

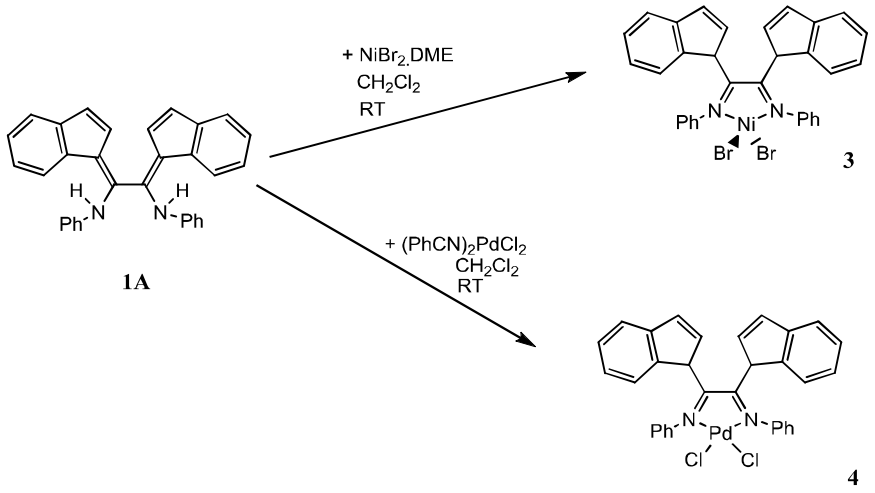

Scheme 3 Reaction pathways towards [{PhNC(C_9H_7)}$_2$NiBr$_2$] (Compound **3**) and [{PhNC(C_9H_7)}$_2$PdCl$_2$] (Compound **4**)

Characterisation of compound **3** by elemental analysis shows agreement with the calculated values for [{PhNC(C_9H_7)}$_2$NiBr$_2$]. The ^{1}H NMR was broad and un-interpretable, which suggests that this is likely a tetrahedral Ni(II) complex (high spin, d^8, paramagnetic complexes). As the analogous DAB ligand, it is known to be a good π-acceptor and therefore induces a large field splitting that should favour the square planar geometry. However, relatively bulky substituents, such as bromine, can remove this preference because groups in a tetrahedral environment are further apart in space than in a square planar geometry. In fact, most [NiBr$_2$(DAB)] complexes are tetrahedral due largely to this steric factor, and numerous examples have been reported [1]. Importantly for polymerisation abilities, these complexes once activated by MAO, thus forming [NiMe(DAB)(solvent)]$^+$, present a square planar geometry, as the case for the derivative [{(2,6-C_6H_3(i-Pr)$_2$)NC(Me)}Ni(Me)(OEt$_2$)]$^+$[B(C_6F_5)$_4$]$^-$ [1]. Thus it was expected a tetrahedral geometry for the diimine form of **4**, [{PhNC(C_9H_7)}$_2$NiBr$_2$], as well as its isomer incorporating ligand in **1B** form. This feature was expected to influence the magnetic properties of this compound, i.e. to induce paramagnetism. The ^{1}H NMR spectrum (CD_2Cl_2) shows a set of broad unresolved resonances between δ 7.3 and 6.1 ppm possibly due to coupling to the paramagnetic centre thus confirming the expectation.

The solid state magnetic moment was determined from magnetic susceptibility studies on a SQUID instrument at a field strength of 1000 G over a range of temperatures, shown in Figure 6. As expected for a pseudo-tetrahedral d^8 complex with a T1 ground state, a large variation was observed between 0 K, where μeff ≈1.7 BM, to ambient temperatures, where μeff ≈ 3.0 BM. This is because the perturbation produced is much smaller than kT (where k =Boltzmann constant, T= Temperature in K). The sample contained no ferromagnetic impurities. This provides further confirmation that the d_8 Ni(II) centre is placed in a tetrahedral environment.

In the low resolution FAB$^+$ mass spectrum signals, which exhibited the expected isotropic pattern, were assigned to: [PhNC(C_9H_7)]$^{2+}$, [{PhNC(C_9H_7)}$_2$Ni]$^+$ and [{PhNC(C_9H_7)}$_2$NiBr]$^+$. The peak for the molecular ion, [{PhNC(C_9H_7)}$_2$NiBr$_2$]$^+$ was not present, but that of a dimer with M/z = 1229.2. The fact that, in the FAB MS spectrum, a peak corresponding to a dimer with M/z = 1229.2 is detected, and the monomeric ion [{PhNC(C_9H_7)}$_2$NiBr$_2$]$^+$ is absent, may point out that the solid state structure of these Ni(II) complexes correspond to neutral dimers, in which 2 Cl atoms are bridging the two Ni(II) atoms (*vide infra*).The IR spectrum did not confirm the complete loss of the N-H bonds: the diagnostic peak at 3356 cm^{-1} was much broader than for the free ligand and there is a strong, broad band centred at 1594 cm^{-1} (higher than that observed in the free ligand, at 1588 cm^{-1}), linked to a likely C=N bond rather than a delocalised C-N(H): overall this analytical data is suggesting that although the reaction occurred, the presence of the NH functionality may well still remain in the final composition, therefore the formation of a Brookhart type complex as the sole isomer cannot be predicted. Given the good match of the elemental analysis, and the expected mass spectrometry fragments, it is likely that the compound displays a number of isomers that could not be separated, and likely some of these are supported by the enamine ligand form **1B** rather than **1A**, analogous to those shown in Scheme 4 and 5 below for Pd(II) analogous systems.

By reacting [PhN(H)C(C_9H_6)]$_2$ with [(PhCN)$_2$PdCl$_2$], formation of a Pd(II) complex of square planar geometry was expected, since, with few exceptions, the co-ordination of Pd(II) is square planar and a search in the CCDC showed that virtually all 4-coordinated DAB-supported [Pd(II)] complexes are displaying this geometry. Thus it was expected that the target complex [{PhNC(C_9H_7)}$_2$PdCl$_2$] would be of square planar geometry too. The elemental analysis of the product was consistent with the proposed structure in scheme above for 4, showing some close agreement with the calculated values. The low resolution FAB$^+$ mass spectroscopy showed signals, which exhibited the expected isotropic pattern, that could be assigned to the following species: [PhN(H)C(C_9H_6)]$^{2+}$, [{PhNC(C_9H_7)}$_2$Pd]$^+$, [{PhNC(C_9H_7)}$_2$PdCl]$^+$ and included the molecular ion [{PhNC(C_9H_7)}$_2$PdCl$_2$]$^+$ and particularly, that of M+Na$^+$ ion with correct isotopic pattern, centred at 635.1/636.1/637.1. However, as before, the presence of a broad peak centred at 3324 cm^{-1} in the IR spectrum does not confirm the complete loss of the N-H bonds and the ^{1}H NMR (CD_2Cl_2) including VT NMR showed a mixture of products.

Multiple sets of resonances between 7.7 and 6.1 ppm were observed, together with peaks in the range δ 5.0 to 2.5 ppm. The ^{13}C {^{1}H} NMR (CD_2Cl_2) spectrum exhibits more peaks than the expected 16 due to the number of inequivalent carbons in the structure given in Scheme 3. No signals due to starting material appear in either spectra. Analysis of the ^{1}H NMR spectrum, in conjunction with $^{13}C\{^{1}H\}$, ^{1}H-^{1}H COSY and the ^{1}H-^{13}C HSQC NMR, led to some resonances outside the aromatic region being assigned to protons of several likely isomers for 4 shown in Scheme 4. A triplet at δ 4.55 ppm is assigned to H_a, coupling to inequivalent H_b and H_c ($^{3}J_{ab}$, $^{3}J_{ac}$ = 7 Hz). A pair of a doublet of doublets are observed at δ 2.77 and δ 2.59 ppm corresponding to H_b and H_c, coupling with each other and H_a ($^{2}J_{bc}$ = 50 Hz). The ^{1}H-^{13}C HSQC NMR (CD_2Cl_2) spectrum confirmed the presence of the CH_2 fragment. However, resonances observed that could not be assigned, in particular a doublet at δ 4.94 ppm and a doublet of doublets at δ 3.18 ppm, led to the following hypothesis.

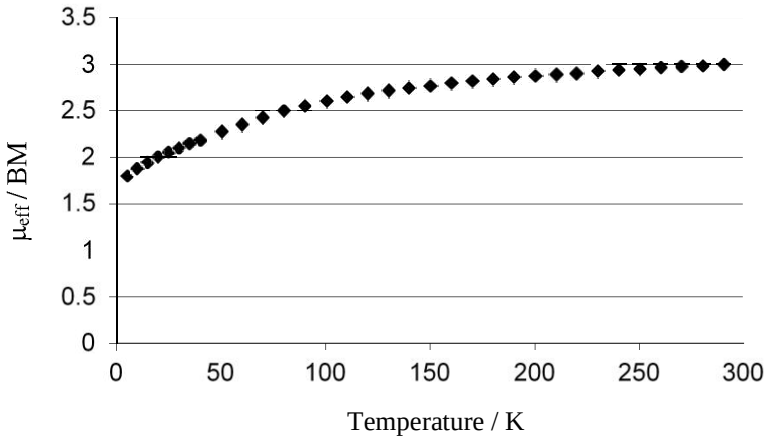

Figure 6. Variable temperature plot of μeff for [{PhNC(C_9H_7)}$_2$$NiBr_2$] at 1000 G

The behaviour of acidic protons, such as N-H, is far from predictable in solution, especially in the presence of halides, i.e. from [$(PhCN)_2PdCl_2$]. Although it has been expected that the N-H protons will migrate to the indenyl ring to give the proposed structure for 4, a number of side reactions are also possible and Scheme 4 outlines the some of the possibilities backed by the spectroscopic data and literature publications so far. Interestingly, the IR spectroscopy in solid state showed only broad resonances in the 3424 cm^{-1} region, and an intense, double band at 1578.0 cm^{-1}, which may well account for the formation of the desired diimine compound [{PhN=C(C_9H_7)}$_2$$PdCl_2$]. Di-enamine and diamide complexes of Pd(II) are well known [45] and the possibility of formation of oligomers [46], such as the examples given below in Scheme 5, cannot be discounted. It can be seen that all these products mentioned are consistent with both analytical purity and mass spectrum species observed for Pd complex **4** (Scheme 4), and, for this compound, intense resonances in the ^{1}H NMR spectrum are assignable to a symmetric species such as the desired α-diimine compound. In view of the IR spectrum, which shows the presence on N-H bonds the possibility that an impurity in the NMR such as a complex supported by a coupled ligand, e.g. a coupled complexed related to form **1A** may well be formed additionally to the expected products: this should not be discounted as Pd(II) is known to catalyse the activated C-C bond coupling reactions.

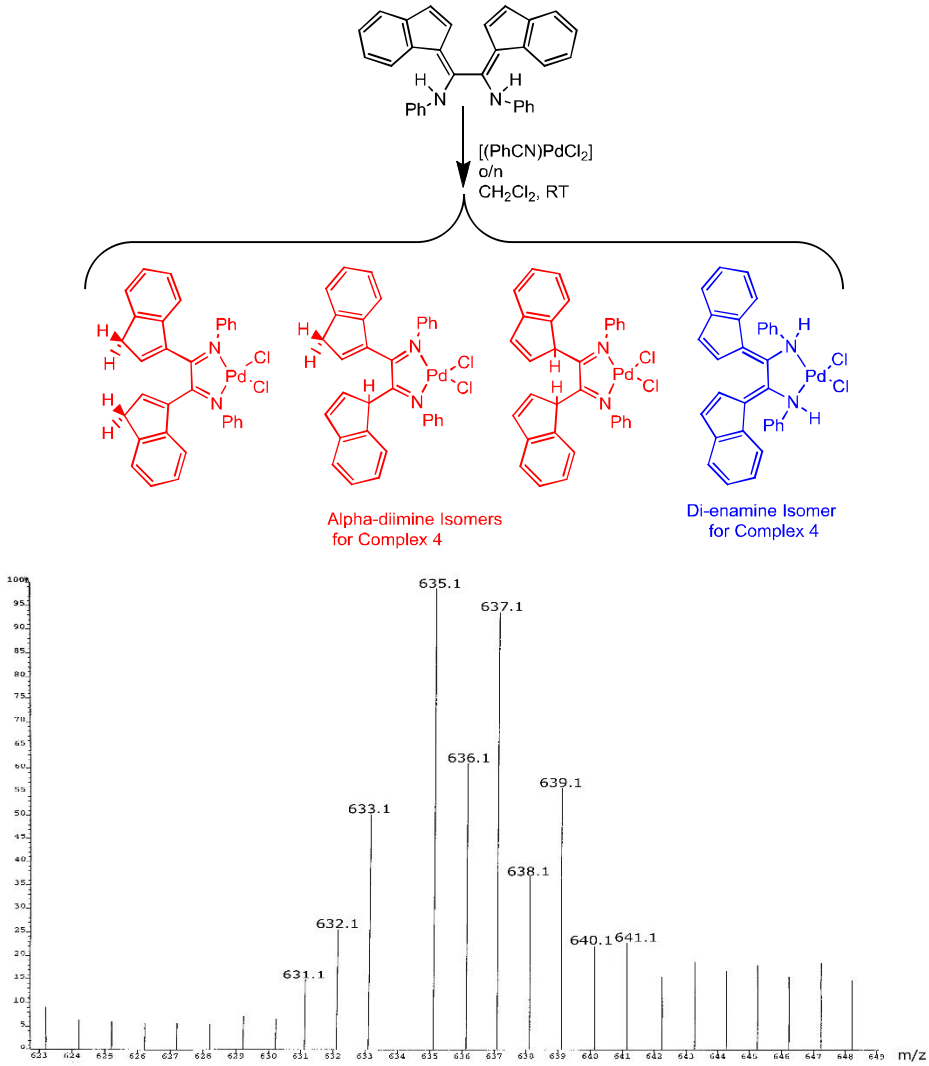

Scheme 4: Possible monomeric isomers formed as products of the reaction between $[(PhCN)_2PdCl_2]$ and Ligand **1B** and corresponding FAB^+ m/z ion for $[M+Na]^+$.

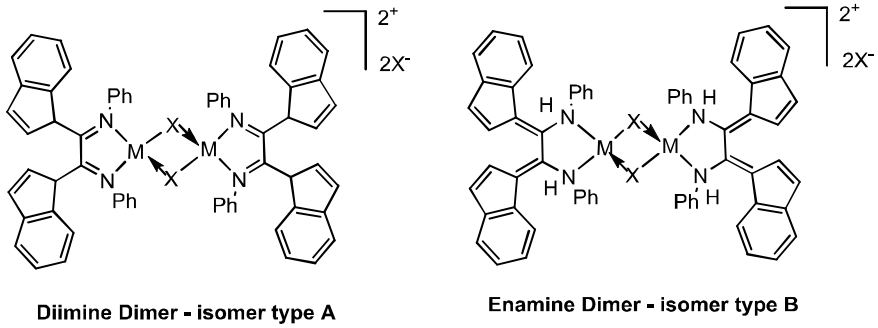

Scheme 5: Possible oligomers for compound **3** and **4**: diimine based (type **A**) and di-enamine based (type **B**). A further set of isomers supported by mixed imine-enamine ligands (type **C**) could also be envisaged, and are not shown, for simplicity.

We were intrigued by the possible structures for (**3**) and (**4**) in the absence of single crystals of suitable quality for an X-ray diffraction study. A detailed search in CCDC database (2016) revealed that there are several example of Ni which exhibit dimeric forms,

with two bromine or two chlorine centres bridging the two Ni(II) atoms [47-52] whereby in these dimers the metal centres are penta- or hexa- coordinated. However, the crystal structures where Ni dimers are held together with 2 Br or Cl atoms bridging the metal centres and simultaneously tetracoordinated nickel(II) have not been found thus far. In these common examples, five and/or six coordination positions are occupied by bromide atoms [50-54] or solvent molecules, e.g. DMF or water molecules [47-49] (Scheme 6). This may point out that the solid state structure of our Ni(II) complexes may well correspond to neutral dimers, in which 2 Br atoms are bridging the two Ni(II) atoms, and in which the Nickel ions are pentacoordinated, with other bromide atom in the fifth coordination position, such as *[{PhNC(C_9H_7)}$_2$NiBr$_2$]$_2$*, in analogy with the complexes previously reported and from which the most closely related species are (IV)-(VII) in Scheme 6 shown below [50-54]. This is in agreement with the fact that, in the FAB MS spectrum, a peak corresponding to a dimer with M/z = 1229.2 is detected, and the monomeric ion [{PhNC(C_9H_7)}$_2$NiBr$_2$]$^+$ is absent.

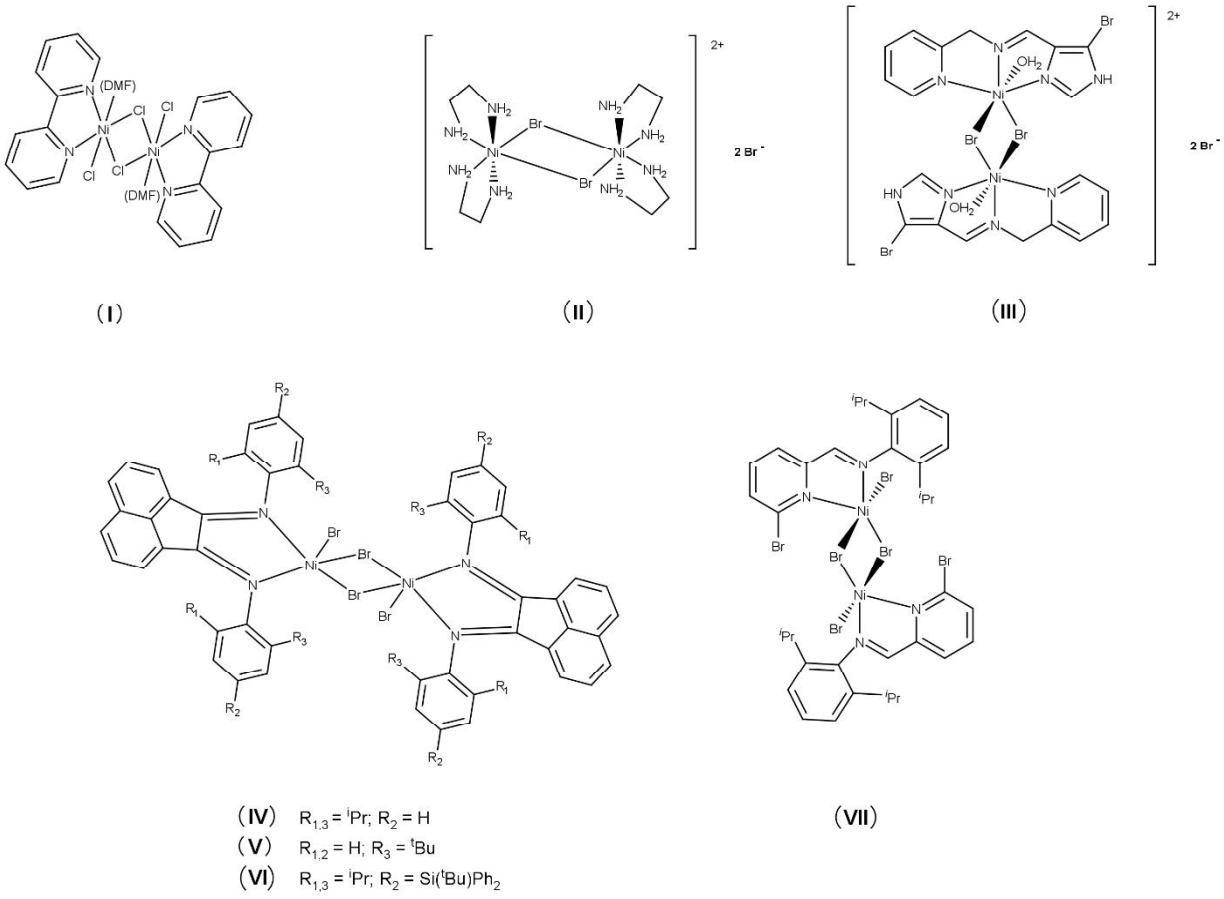

Scheme 6. Examples of related dimeric Ni(II) complexes found in the CCDC: **(I)** Di-μ-chlorido-bis-[(2,2′-bi-pyridine-κ^2N,N')chlorido(*N*,*N*-di-methyl-formamide-κ^0)nickel(II)] [47]; **(II)** Di-μ-bromo-bis-[bis-(1,2-diamino-ethane-κ^2N,N)nickel(II)] dibromide [48], **(III)** Di-μ-bromo-bis-{aqua-[(5-bromo-1H-imidazol-4-ylmethyl-ene)(2-pyridylmeth-yl)amine-κ^3N,N',N'']nickel(II)} dibromide [49], **(IV)** Di-μ-bromo-bis[N,N'-(2,6-diisopropylphenyl)imino]acenaphthene}bromonickel [50], **(V)** Di-μ-bromo-bis[N,N'-(6-tert-butylphenyl)imino]acenaphthene}bromonickel [51], **(VI)** Di-μ-bromo-bis[N,N'-(4-tert-butyl-diphenylsilyl-2,6-diisopropylphenyl)imino]acenaphthene}bromonickel [52], and **(VII)** Di-μ-bromo-(2,6-bis(1-methylethyl)-N-[(6-bromo-2-pyridinyl)-methylene]phenylamine)bromonickel [53].

Polymerisation tests for 3 and 4

The metal complexes as-isolated from the reactions shown in Scheme 3 were tested with co-catalyst MAO (methylaluminoxane) for catalytic activity towards the polymerisation of ethene as described in Experimental section. The activity of the MAO was initially tested using a known ethene polymerisation catalyst, Cp_2ZrCl_2, with known activity [55]. An activity of 1.411 x 10^6 g PE mol M h^{-1} was found using as benchmark the well-known Cp_2ZrCl_2 and MAO as the precatalyst and activator *in situ* system, which was tested in the same autoclave. The MAO was thus considered active as this value is sufficiently close to the reported activity of 3.57 x 10^6 g PE mol M h^{-1}. The toluene solution of [{PhNC(C_9H_7)}$_2$NiBr$_2$] in the presence of excess MAO was tested over one hour in the conditions given below. Formation of solid, insoluble polymer was not observed. Deactivation of the catalyst, with an ethanol/HCl mixture, afforded a toluene layer of oily appearance. A 10 mL sample taken and passed through a pipette containing silica to remove the metal, denoted sample (i).

The remainder was reduced on the rotary evaporator to ≈ 15mL and then passed through a pipette containing silica to remove the metal to generate the fraction denoted sample ii, which was concentrated under the reduced pressure. These samples were analysed using gas chromatography and the results are given in Table 2. As expected, the species observed in sample (i) with retention times and therefore boiling points below that of toluene, do not appear in sample (ii), which was the more concentrated GC sample. The species with retention times of 1.93, 3.75 and 9.35 minutes observed in sample (i) and 9.58 minutes in sample (ii) could infer the presence of a species' generated under the catalysis conditions, i.e. ethylene oligomers.

Table 2. Gas Chromatography results * = toluene ** = ethanol. Toluene with retention times of around 6 minutes can be seen in all samples as the most dominant compound as this was the solvent media used. Ethanol, as part of the quenching solution, is expected and is observed to have a retention time of around 3 minutes.

Sample Number	**Retention Times (minutes)**	**Concentration (%)**
Dry toluene	5.55	99.420
Ethanol	3.03	100.00
GC Sample (**i**)	1.93 2.83** 3.75 6.05* 9.35	0.037 0.844 0.151 97.987 0.021
GC Sample (**ii**)	6.08 9.58	99.855 0.145

A highly-cited pioneering paper by Brookhart and Svejda [15] describes the ethene oligomerisation properties of a number of α-diimine nickel(II) catalysts. It has been reported that when α-diimines without bulky *ortho* substituents at the aryl groups are used, the resulting Ni(II)-based systems produce ethylene oligomers. Ethene polymerisation [(DAB)NiX_2] catalysts have bulky *ortho* substituents placed in axial sites to the plane of the aryl ring which effectively retard the rate of chain transfer relative to chain propagation. Without these, in such complexes as [{$(C_6H_4$(p-Me))NC(Me)$\}_2NiBr_2$], chain transfer *via* β-elimination is not retarded, resulting not in polymers but shorter oligomers. Thus [{$PhNC(C_9H_7)\}_2NiBr_2$], without bulky aryl *ortho* substituents, could be expected not to give polymers but lower mass oligomers, which in general are soluble in toluene. The preliminary results from the gas chromatography experiment suggest that this may indeed be the case but further experiments would be required, such as gas chromatography mass spectroscopy, to fully characterise the activity and products of such systems. The toluene solution of proposed [{$PhNC(C_9H_7)\}_2PdCl_2$] with MAO was likewise tested yielding a small amount of black solid, likely palladium metal because of its colour and appearance. The Pd(II) species isolated previously is only sparingly soluble in toluene. The toluene layer on quenching was analysed in the gas chromatograph showing only a peak due to toluene with retention time of 6.02 minutes. The inferred lack of activity from this preliminary experiment may be due to the deficiency of [{$PhNC(C_9H_7)\}_2PdCl_2$] in the portion tested, through decomposition or the presence of a mixture of Pd(II) species (see earlier discussion), but may also reflect the fact that palladium analogues of Brookhart-type nickel catalysts are invariably less active catalysts [56].

Towards design and synthesis of bulky analogues [ArNC(Ind)]$_2$, Ar = 2,6- $Me_2C_6H_3$, (5) and 2,6- $iPr_2C_6H_3$, (6)

As the di-enamine form (**1B**) of the compound [PhN(H)C(Ind)]$_2$ had been shown to be the preferred isomer, rather than the diimine [PhNC(Ind)]$_2$, the synthesis of analogues of this ligand incorporating bulky substituents in the *ortho* positions of the aryl ring was also attempted, aiming to probe the steric effect on the choice of di-enamine *vs* diimine formation. It was expected that the imine form of the compound would be favoured with increase bulkiness of the amine substituent, which in turn would lead to favouring the co-ordination to metal to form α-diimine complexes. In addition, these bulky substituents are known to favour polyolefin formation rather than oligomers in ethylene polymerisation catalysis, due to their steric protection of the axial sites modulating the rate of β-elimination of the growing chain. Two equivalents of lithium indenide were added to one equivalent of [ArN=C(Cl)]$_2$ in Et_2O (Ar = 2,6-$Me_2C_6H_3$) or in THF (Ar = 2,6-^{i}PrC_6H_3). In both cases, the reaction mixture was stirred for 60 hours starting at -78 ºC, and allowing these to reach the room temperature, and in both cases the reactions proceeded with yields no higher than ca 20%. For the case where Ar = 2,6-$Me_2C_6H_3$, the ^{1}H NMR (CD_2Cl_2) spectroscopy showed three sets of resonances assignable to the isomers of types **A**, **B** and **C** of the desired product and whoch suggested the formation of the bis-indenyl-diimine product alongside enamine-containing species, with the proposed structures shown in Scheme 6. These were found to be in a ratio of approximately 1:2:1 by integration in ^{1}H NMR spectrum. There were strong similarities between this NMR spectrum and that of the literature data concerning a recently reported substituted alpha-diimine *[ArN=C)(Fluorenyl)]$_2$, Ar = 2,6- $Me_2C_6H_3$* [57]. A variable temperature experiment, performed between room temperature and -40 ºC did not indicate any change of the appearance of the ^{1}H NMR spectra with temperature, so did not support the theory that these three species are in exchange within this temperature range.

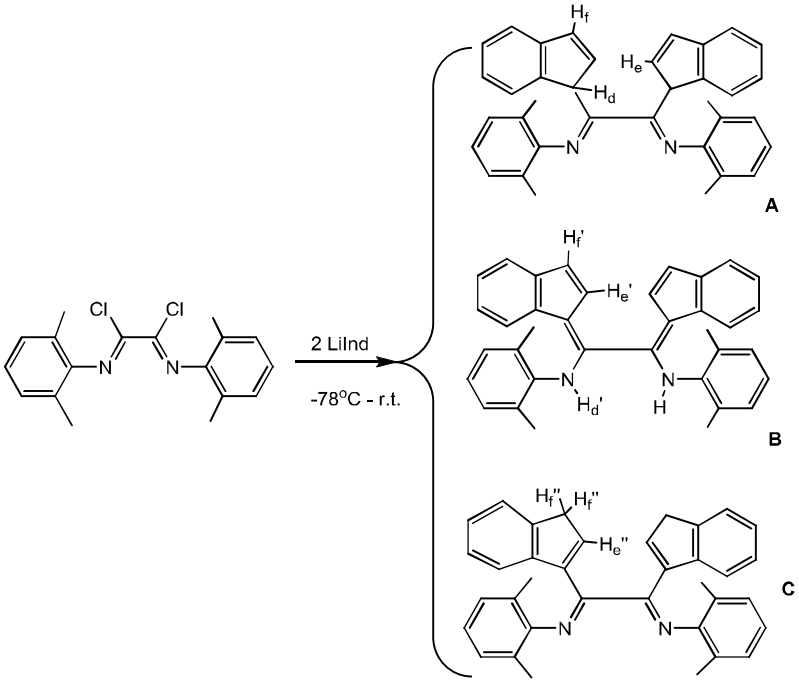

Scheme 7 Reaction between $\{(2,6\text{-}C_6H_3Me_2)N{=}C(Cl)\}_2$ and LiInd to give compound **5** as a mixture of isomers of types **A**-**C**

The following ^{1}H NMR data was used in support of the hypothesis for the presence of the proposed species shown in Scheme 7:

- For species **5A**, a doublet at δ 3.62 ($^2J_{HH}$ = 1.5 Hz) was assigned to H^d, the double doublet at δ 5.85 ($^2J_{HH}$= 6 Hz, $^2J_{HH}$ = 1.5 Hz) was assigned to H^e and the doublet at δ 5.98 ($^2J_{HH}$ = 6 Hz) was assigned to H^f.
- For species **5B**, H^f was found as a doublet at δ 6.40 ($^2J_{HH}$ = 6 Hz) and a doublet for $H^{e'}$ at δ 6.90 ($^2J_{HH}$ = 6 Hz). The NH proton was assigned to a singlet at δ 6.85.
- For species **5C**, a doublet assigned to the $H^{f''}$ protons was found at δ 3.40 ($^2J_{HH}$ = 2 Hz) and a triplet from $H^{e''}$ at δ 5.88 ($^2J_{HH}$ = 1.5 Hz).

For **5**, the triplet resonances at higher field in the ^{1}H NMR spectrum (δ 2.39, δ 2.27, δ 2.02) were assigned to the methyl protons of $Me_2C_6H_3$ units in species **5A**, 5**B**, and **5C** respectively. The aromatic protons of the (2,6-$Me_2C_6H_3$) group of the isomer **5A** were found at δ 6.45 (a doublet with $^2J_{HH}$=7.5Hz for the *meta* protons) and at δ 6.53 (a triplet with $^2J_{HH}$=7.5Hz for the *para* hydrogen). The remaining aromatic protons of the species **5A**, **5B**, and **5C** are found between δ 7.80 and δ 6.60. Separation of the products could not be achieved due to their similar solubilities in most organic solvents. The presence of the two diimine isomers, **5A** and **5C**, indicates that the possible equilibrium of the type shown in Scheme 1 is shifted towards the formation of the imine isomer for bulky isomers, e.g. when R = Me. However, the presence of some traces of species **5B** in solution still suggests that the use of bulky *ortho*-substituents does not completely prevent the tautomerisation of the imine to the enamine form during the reaction process, as previously seen for $[PhNC(Ind)]_2$ (compound **1**), discussed above.

The analogous reaction was carried out in order to synthesise the isopropyl-substitued, bulkier analogue, $[(2,6\text{-}iPr_2C_6H_3)N{=}C(Ind)]_2$, denoted Compound **6**, as shown in Scheme 8. On removal of solvent from the reaction mixture, a dark green solid was obtained. The ^{1}H NMR spectrum of the green solid shows that this is a mixture of the desired product, **6A**, together with the dienamine isomer **6B**, in the ratio 3:1 by ^{1}H NMR integration. The ^{1}H NMR spectrum was assigned using a ^{1}H-^{1}H COSY experiment. An NOE difference experiment assisted the assignment, showing resonances corresponding to isomers of types **6A** and **6B**.

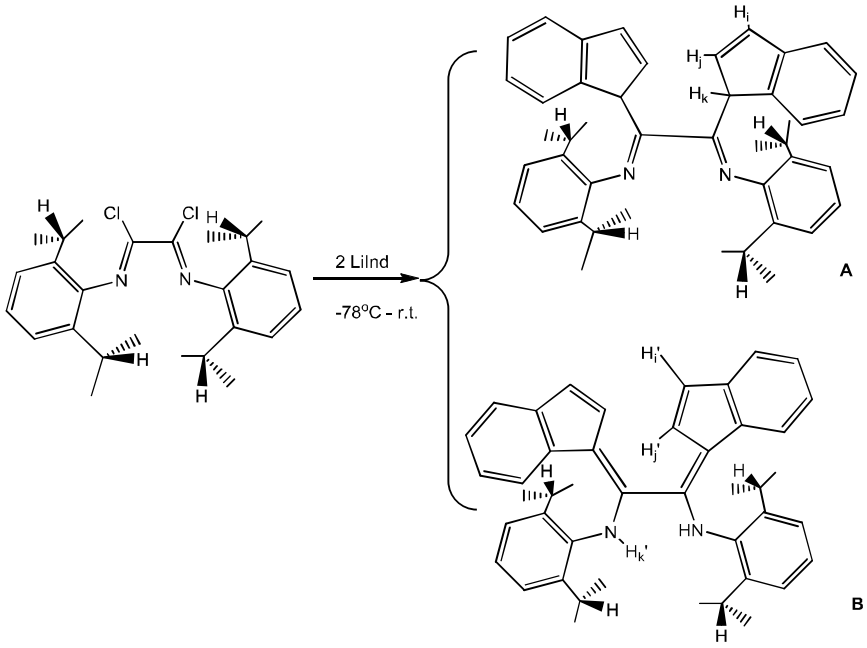

Scheme 8 Reaction between $[(2,6\text{-}iPr_2C_6H_3)N{=}C(Cl)]_2$ and LiInd to give compound **6** as a mixture of isomers

The following resonances which support the hypothesis for the formation of the two species of types **A** and **B** were observed in the ^{1}H NMR spectra of compound 6 and correspond to the labelled, diagnostic, protons shown in Scheme 8:

- For species **A**, H^k was seen as a doublet at δ 3.60 ($^3J_{HH}$=2.2Hz), H^j was observed as a doublet of doublets at δ 7.18 ($^3J_{HH}$=2.0 Hz, $^3J_{HH}$=5.0Hz), and H^i as a doublet at δ 7.32 ($^3J_{HH}$=5.0Hz)
- For species **B**, $H^{j'}$ was seen as a doublet at δ 6.40 ($^3J_{HH}$=5Hz), a broad peak assigned to $H^{i'}$ was seen at δ 6.20 (thought to be broad due to exchange with the NH proton) and the NH resonance observed at δ 6.45 as a singlet which is not seen to be coupled with other resonances in the ^{1}H-^{1}H COSY spectrum

The resonances assigned to the isopropyl C*H* groups were observed at δ 3.20 and δ 2.90 for species **A** and **B** respectively, in the ratio 3:1. Methyl resonances were observed as doublets at δ 1.20 and δ 0.80 for species **A** and **B** respectively. Other resonances were seen in the aromatic region, between δ 8.10 and δ 6.90, and are assignable to the indenyl groups.

The reactions described above indicate that the substitution of the chlorine atoms on the diimine backbone with indenyl groups occurs. However, in contrast to the phenyl analogue (R = H, compound **1**, isomer **1B**), yields are poor, and purification was difficult due to the similar solubility of the isomers obtained. The additional steric hindrance provided by the substituents on the aryl rings is presumably sufficiently large to prevent the tautomerisation reaction from occurring in high yield. However, it can be seen that, as the steric bulk of the *ortho*-substituents increases, so does the yield of the desired diimine adduct in the reaction mixture: with diisopropyl as the *ortho*-substituent, the diimine is the predominant product, with only minor impurities of the dienamine apparent, however the separation of the isomers remains a challenged to be addressed in further experiments. With the appreciation of the fact that the bulky compounds 5 and 6 were present as an inseparable mixture of isomers, their reactivity towards a wide range of group 10 metal salts were tested under analogous consitions applied for the phenyl analogue. Reactions with $[NiBr_2(DME)]$, [PdMeCl(COD)], $[PdBr_2]$ and $[PtCl_2(COD)]$ in toluene, at room temperature or under reflux, all resulted in the isolation of a mixture of metallated species, as evidenced by mass spectrometry and, for the [Pd] and [Pt] species by ^{1}N NMR spectroscopy. The tautomeric equilibrium expected for the free ligands did not seem shifted sufficiently towards formation of one single metal complex either monomeric or dimeric in nature, and our investigations into this rather complex group of molecules are ongoing.

EXPERIMENTAL SECTION

All manipulations were carried out under an atmosphere of dinitrogen using standard Schlenk-line or drybox techniques. The nitrogen was purified by passage over 4Å molecular sieves and BASF R-311 catalyst. Solvents and solutions were transferred using a positive pressure of inert gas through stainless steel cannulae. Filtrations were generally performed using modified stainless steel cannulae fitted with glass fibre filter paper. All glassware and cannulae were dried overnight before use.

All preparations and manipulations were carried out under an inert atmosphere of dried nitrogen using either standard Schlenk techniques or a dry box. Liquids were transferred through stainless steel cannulae (0.5mm-2mm diameter) by excess nitrogen pressure. Unless otherwise stated, filtration was achieved using such cannulae modified to take a glass-fibre filter at one end. Celite™ 545 filtration aid (Koch-Light) was pre-dried at 80°C before use. All glassware and cannulae were dried in an oven at 140 °C.

All solvents were thoroughly deoxygenated before use by repeated evacuation followed by admission of nitrogen. Solvents were pre-dried over molecular sieves and refluxed over the appropriate drying agent (sodium for toluene and tetrahydrofuran, sodium/potassium alloy for diethyl ether and n-pentane, calcium hydride for dichloromethane) under an atmosphere of dinitrogen and collected by distillation. NMR solvents were dried over calcium hydride (dichloromethane, chloroform) at room temperature or molten potassium (benzene, toluene), distilled under vacuum and stored under dinitrogen in Young's ampoules.

^{1}H, $^{13}C\{^{1}H\}$ and $^{31}P\{^{1}H\}$ NMR spectra were recorded either on Varian Unity 500 or Varian Mercury 300 spectrometers and referenced internally to the residual solvent peak relative to tetramethylsilane. The spectra were referenced internally to the residual solvent peak relative to SiMe4 (δ = 0.0). All chemical shifts are quoted in δ(ppm) and coupling constants are given in Hertz (Hz). Infra-red spectra were recorded on a 6020 Galaxy Series FT-IR or a Perkin Elmer 1600 Series FT-IR instrument in the range 4000-400 cm^{-1}. Samples were prepared in the glovebox as pellets in caesium iodide, and data are quoted in wavenumbers (ν, cm^{-1}). Elementary analyses data were obtained from the microanalysis department of the Inorganic Chemistry Laboratory. Mass spectra were obtained using the EPSRC facility of the University of Swansea. Gas chromatography was performed on a Phillips-Pye Unicam P4550 Gas Chromatograph (FID). The chromatograph has a 25 m silica tube capillary column with a polar BP20 polyethylene glycol packing and helium was used as the carrier gas. SQUID analysis was performed on a Quantum Design MPMS-5 Magnetometer. Ferromagnetic contributions to the results were tested for and excluded and corrections for diamagnetic factors in the magnetic susceptibility were made with reference to the literature [58].

Two-photon excitation experiments were performed at the Rutherford Appleton Laboratory following the methodology described by Botchway *et al*. 2008 [59]. A mode locked Mira titanium sapphire laser (Coherent Lasers Ltd, USA), generating 180 fs pulses at 75 MHz and emitting light at a wavelength of 710-970 nm was used for the 2-photon excitation. The laser was pumped by a solid state continuous wave 532 nm laser (Verdi V18, Coherent Laser Ltd), with the oscillator fundamental output of 915 ± 2 nm. The laser beam was focused to a diffraction limited spot through a water immersion ultraviolet corrected objective (Nikon VC x60, NA1.2) and specimens illuminated at the microscope stage of a modified Nikon TE2000-U with UV transmitting optics. The focused laser spot was raster scanned using an XY galvanometer (GSI Lumonics). Fluorescence emission was collected and passed through a coloured glass (BG39) filter and detected by fast microchannel plate photomultiplier tube used as the detector (R3809-U, Hamamatsu, Japan). These were linked via a Time-Correlated Single Photon Counting (TCSPC) PC module SPC830. Lifetime calculations were obtained using SPCImage analysis software (Becker and Hickl, Germany) or Edinburgh Instruments F900 TCSPC analysis software.

Single crystal X-ray diffraction.

Data collection

In each case, a single crystal was selected under an inert atmosphere, encased in perfluoro-polyether oil, and mounted on the end of a glass fibre. Data was first collected on an Enraf-Nonius Mach-3 Serial diffractometer using monochromatic Cu K_α radiation at λ = 1.54184Å. Data frames were processed using the RC93 [60] program. The data collections for compounds **1B** and **2** were performed again, using an Enraf-Nonius DIP2000 image plate diffractometer with graphite monochromated Mo Kalpha radiation (λ = 0.71069 Å). In each case the same structure was obtained, and the best data sets are reported. Corrections for Lorentz and polarisation effects were performed. For structure solution and full-matrix least-squares refinement the WINGX-v2014 suite of programs was used [61]. All non-hydrogen atoms were refined with anisotropic displacement parameters. C-H hydrogen atom were placed onto calculated positions and refined riding on their parent atom. All hetero atom hydrogen atoms have been located in the difference Fourier map and were refined freely. The program MERCURY [62] was employed for the graphics used hereby. Full experimental details are included in the ESI. CCDC 1474229 contains the supplementary crystallographic data for compound **1B** and CCDC 1474223 contains the supplementary crystallographic data for compound **2**.

Precursors synthesis:

The intermediate $Ph_2PC(=O)\text{-}C(=O)PPh_2$ [63] and PhN=C(Cl)C(Cl)=NPh [64] were prepared via a modification of the literature. Also, the precursors $(2,6\text{-}Me_2C_6H_3)N=C(Cl)C(Cl)=N(2,6\text{-}Me_2C_6H_3)$ [57] and $(2,6\text{-}^{i}Pr_2C_6H_3)N=C(Cl)\text{-}C(Cl)=N(2,6\text{-}iPr_2C_6H_3)$ were prepared according to literature [65].

Alternative method for the preparation of $[PhN=C(Cl)]_2$

Approximately 100 mL toluene was transferred to a 3-necked round-bottomed flask fitted with a condenser containing PCl_5 (50g, 0.24 mol) and $[PhN(H)C(O)]_2$ (25g, 0.104mol). The mixture was refluxed for 3 hours affording a yellow solution, which was cooled to room temperature and filtered to remove insoluble material.

The solvent was removed under reduced pressure until a large amount of bright yellow solid was formed. The suspension was then filtered to afford a bright yellow solid as the product, $[PhN=C(Cl)]_2$. The yellow filtrate was reduced *in vacuo* enabling more product to be isolated from the resulting suspension. This procedure was repeated again giving overall three portions of $[PhN=C(Cl)]_2$; 20.2g, total yield = 69.6 %. ^{1}H NMR (CD_2Cl_2) δ 7.48 (t, 2H, *m*-C_6H_5) , δ 7.30 (t, 1H, *p*-C_6H_5), δ 7.12 (d, 2H, *o*-C_6H_5) ppm. Elemental Analysis: Found C, 59.95; H, 3.43; N, 9.84; Cl, 24.35%. Calc. C, 60.67; H, 3.64; N, 10.11; Cl, 25.58%. Selected IR data (nujol): V(C=N): 1664 cm^{-1}

Synthesis of Compound 1:

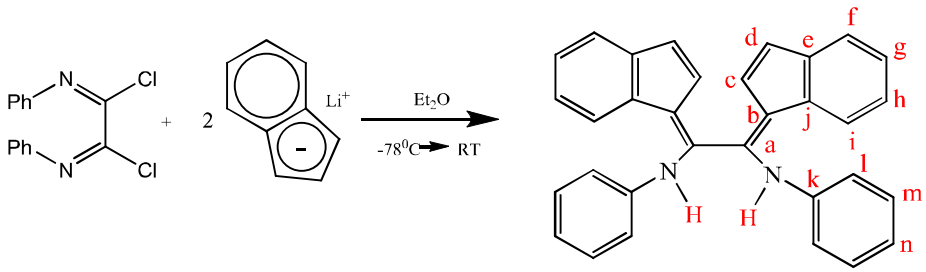

Scheme 9: Preparation of $[PhN(H)C(C_9H_6)_2]_2$, isomer **1B**

Method 1

Step1: Preparation of lithium indenide

Indene (25mL, 0.2143mol) was transferred into a large Schlenk vessel and mixed with approximately 500 mL petroleum ether (40 - 60°C). The solution was bubbled through with nitrogen to remove any air from the indene used. 75.2 mL of nBuLi (2.5M, 0.188mol) was added dropwise over 30 minutes and the solution was stirred for a further 18 hours keeping at room temperature. The white suspension was filtered and washed with 2 x 20mL petroleum ether (40-60°C) giving the off-white lithium indenide on drying *in vacuo*, and was used for the next step without further purification.

Step 2: Preparation of the $[C_6H_5NH-C(C_9H_6)-C(C_9H_6)-NHC_6H_5]$

A stirring yellow suspension of $[C_6H_5N=C(Cl)-C(Cl)=NC_6H_5]$ (2.81g, 24.6mmol) in diethylether (50 mL) at –78 ºC was treated with a pale-yellow suspension of LiC_9H_7 (6.0g, 49.1mmol) in diethylether (30mL). The reaction mixture was warmed to the room temperature and stirred overnight. After 21 h. of stirring, the solvent was removed and the residue was extracted with CH_2Cl_2 (30 mL) to afford a dark-red solid, which was washed with ether (20mL) followed by pentane (10mL) to afford a red solid. Yield: 4.48g, 60.08%.

Method 2

The compound $[PhN=C(Cl)]_2$ (5.54 g, 0.02 mol) was weighed out into a Schlenk vessel and dissolved in 100 mL Et_2O at -78 ºC. Likewise, lithium indenide (4.88g, 0.04mol) was dissolved in 100 mL Et_2O, cooled to -78 ºC and added dropwise over 30 minutes to the $[PhN=C(Cl)]_2$ solution vessel. The colour initially went a dark red, but over 18 hours of stirring while allowing to reach room temperature, became a bright red suspension.

The Et_2O was removed under reduced pressure and the bright red residue extracted into 100 mL CH_2Cl_2. The solution was filtered leaving a residue of LiCl, which was re-washed in 25 mL CH_2Cl_2, to afford a filtrate containing the product.

Solvent was removed from the filtrate leaving a bright red powder. The powder was then washed in approximately 100 mL Et_2O at -78 ºC, giving a suspension. This was filtered giving the desired product, a bright red powder as residue. Solvent was removed from the filtrate, which still contained some of the desired product. The bright red solid was washed in 50 mL Et_2O at -78°C and filtered, giving more product as the residue; 3.97g, total yield = 45.5 %. Elemental Analysis: Found (%): C, 87.12; H, 5.91; N, 6.22. Calculated (%): C, 88.04; H, 5.54; N, 6.42. Selected IR data (CsI pellet(cm-1)): 3396(NH), 3056m, 1576s, 1489s, 1446s, 1392s, 1350s, 1302s, 1266s, 1196s, 1152m, 1110m, 1072m, 1026m, 934m, 900m, 866m, 750s, 726s, 690s, 524m, 448s, 414s. Mass spectrometry TOF EI^+: found $[M]^+$: 436.2083. ^{1}H NMR, C_6D_6, 500 MHz: 6.07(s, 2H, NH), 6.47(m, 4H, l-Ph), 6.59(d, 2H, J= 5.5Hz, c or d-Ind), 6.66(t, 2H, J= 7.5Hz, n-Ph), 6.69(d, 2H, J= 5.5Hz, c or d-Ind), 6.78(m, 4H, m-Ph), 7.00(m, 2H, h or g-Ind), 7.13(m, 2H, h or g-Ind), 7.28(d, 2H, J= 7.0, f or i-Ind), 7.60(d, 2H, J= 7.0, f or i-Ind). $^{13}C\{^1H\}$ NMR, C_6D_6, 125 MHz: 118.5(s, l-Ph), 121.9(s, f or i-Ph), 122.6(s, f or i-Ph), 122.7(s, f or i + n-Ph), 124.8(s, g or h-Ph), 127.0(s, g or h-Ph), 127.1(s, c-In), 129.1(s, m-Ph), 130.0(s, d-In), 141.2 (s, k-Ph), 131.0, 134.4, 138.3, 144.2 (4 quaternary carbon, a,b,e,j), ^{1}H NMR, CD_2Cl_2, 500 MHz: 6.52(s, 2H, NH), 6.67(m, 4H, l-Ph), 6.67 (d, 2H, *J*= 5.4Hz, c-Ind), 6.96(t, 2H, J= 7.4Hz, n-Ph), 6.72 (d, 2H, J= 5.4Hz, d-Ind), 7.13(m, 4H, m-Ph), 7.18(m, 2H, h-Ind), 7.25(m, 2H, g-Ind), 7.43(d, 2H, J= 7.5, f-Ind), 7.82(d, 2H, J= 7.5, i-Ind). $^{13}C\{^1H\}$ NMR, CD_2Cl_2, 125 MHz: 118.78(s, l-Ph), 121.72 (s, f -Ph), 122.33(s, i-Ph), 122.95 (s, n-Ph), 124.50 (s, h-Ph), 126.02 (s, d-In), 126.75(s, g-Ph), 129.23(s, m-Ph), 129.95 (s, b, quaternary), 130.01(s, c-In), 134.13 (s, j-In),

138.68 (s, a, quaternary), 140.87 (s, k-Ph), 143.86 (s, e-In). Coupling constants (Hz): $^3J_{Hm-Hn}$ =7.4, $^4J_{Hl-Hn}$ = 1.1, $^3J_{Hm-Hl}$ = 8.4, $^3J_{Hc-Hd}$=5.4 Hz, $^4J_{Hf-Hd}$=0.6 , $^5J_{Hi-Hd}$ =0.6 Hz, $^3J_{Hi-Hh}$ =7.6, $^4J_{Hg-Hi}$=1.1, $^3J_{Hg-Hh}$ = 7.5, $^3J_{Hf-Hg}$=7.5, $^4J_{Hf-Hh}$ = 1.1, $^5J_{Hf-Hi}$ = 0.7.

Preparation of Compound 2

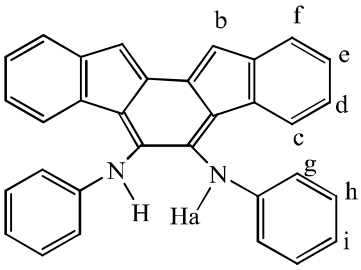

Reaction between [PhN(H)C(Ind)]$_2$ (Compound 1B) and [PtMe$_2$(COD)] leading to isolation of Compound **2** proceeded as follows.

A cooled (-78°C) solution of [PhN(H)C(Ind)]$_2$ (0-1009, 0.2 mmol) dissolved in toluene (50 mL) was added dropwise to a cooled solution (-78°C) of [PdMe$_2$(COD)] precursor, (0.076g, 0.2 mmol) in toluene (50mL). The orange-red reaction mixture was allowed to return to room temperature with stirring overnight, after which there was no observable colour change. The reaction mixture was refluxed for 3 hours. A platinum mirror was observed after 1 hour. Filtration of the resultant mixture yielded an orange solution, which gave an oily orange solid on removal of volatiles under reduced pressure, and a back precipitate likely platinum particulates. Recrystallisation in pentane (20mL) afforded an oily orange solid from the filtrate and the desired product Compound 1 as an orange-brown solid. Yield= 0.045g, 35.4%. ^{1}H NMR, CD_2Cl_2, 500 MHz: 7.60 (d, 1H, H_c or H_f, ^2J = 7.5 Hz), 7.54 (d, 1H, H_c or H_f, ^2J = 7.5Hz), 7.46 (t, 1H, H_d or H_e, ^2J = 8.0Hz), 7.36 (t, 1H, H_d or H_e, ^2J = 8.0 Hz) 7.26 (s, 1H, H_b), 6.63 (t, 2H, H_h, ^2J = 7.5Hz), 6.41 (d, 2H, H_g, ^2J = 7.5Hz), 6.30 (t, 1H, H_i, ^2J = 7.5Hz), 5.68 (s, 1H, H_a). ^{13}C NMR, CD_2Cl_2, 125 Mhz: 143 (C_f or C_c), 138 (C_f or C_c), 136 (C_d or C_e), 130 (C_d or C_e), 127 (C_b), 129 (C_a), 122 (Ci), 121 (C_g), 110 (C_h). Elemental Analysis $C_{32}H_{22}N_2$ % Found (Calculated) C 87.13 (88.45), H 5.31 (5.10), N 5.25 (6.45). Mass spectrometry TOF EI$^+$: found [M]$^+$: 434.1793 (calculated accurate mass for $C_{32}H_{24}N_2$: 434.1783)

Preparation of [{PhNC(C_9H_7)}$_2$NiBr$_2$], Compound 3

Approximately 200 mL CH_2Cl_2 was added to a round-bottomed flask containing [NiBr$_2$(DME)] (1.34 g, 0.0043 mol) and [PhN(H)C(C_9H_6)]$_2$ (2.087 g, 0.0047 mol) The solution was stirred at room temperature overnight. After 18 hours of stirring, the volatiles were removed to afford an oily brown solid which was washed with 100mL (50 mL in portions) Et_2O to give a light brown powder. This powder was redissolved in approximately 25 mL CH_2Cl_2 and transferred to a Schlenk vessel containing approximately 150 mL pentane. A precipitate was formed upon addition and the solution was filtered giving as light/brown beige powder as product. Yield: 1.17 g, 41.5%. Elemental Analysis Found (%): C, 58.01; H, 3.85; N, 4.16; Br, 24.78; Ni, 8.33. Calculated (%): C, 58.67; H, 3.69; N, 4.28; Br, 24.40; Ni, 8.99. Mass spectrometry TOF EI$^+$: found [M]$^+$ M/z (intensity%): 436(68) [Ligand]$^+$, 494/496 (39) [M-2Br]$^+$, 573/575 (72) [M-Br]$^+$

Reaction between [(PhCN)$_2$PdCl$_2$] and [PhN(H)C(C_9H_6)]$_2$, Compound 4

A similar procedure as described in above for compound **3** was followed for the synthesis of **4**. The complex [(PhCN)$_2$PdCl$_2$] (0.58 g, 0.0015 mol) was reacted with [PhN(H)C(C_9H_6)]$_2$ (0.726 g, 0.00163 mol) to afford a dark orange-brown powder as the product denoted compound **4**, with the proposed general formula [{PhNC(C_9H_7)}$_2$PdCl$_2$], likely a mixture of diamine/di-enamine isomers, with the most significant of the ^{1}H NMR resonances given in the main text. Reaction yield: 0.52g, 56.5%. Elemental Analysis: Found C, 60.52; H, 4.06; N, 4.08; Cl, 10.02; Pd,15.07%. Calc. C, 58.67; H, 3.69; N, 4.28; Cl, 11.55; Pd, 17.33%. Mass spectrometry TOF EI$^+$ M/z (intensity%): found [M]$^+$: 436(100) [Ligand]$^+$, 540/542 (27) [M-2Cl]$^+$, 577/579 (28) [M-Cl]$^+$ 613 (15) [M]$^+$.

Polymerisation tests

Ethene was purified by passage through 4 Å molecular sieve. Polymerisations were carried out in a Fischer-Porter reactor equipped with a magnetic stirrer under conditions similar to those employed by Kaminsky *et al*. [55] Toluene (200 mL) was transferred into a Fischer-Porter bottle, which was then connected to the ethene supply and filled with the gas. Methylaluminoxane (MAO) in toluene (9.4 mL) was then added, the ethene pressure increased to 2 bar and the mixture stirred at room temperature until saturated with ethene. Meanwhile, 0.6 mL of MAO was added to 10 mL of the catalyst/ toluene solution (6.25 x 10^{-6} mol of transition metal in total) and stirred for 15 minutes pre-activation. The catalyst-MAO mixture was added quickly to the Fischer-Porter bottle, and the mixture stirred vigorously at room temperature under 2 bar pressure of ethene for 1 hour. The reaction was quenched by venting the ethene and pouring the contents of the bottle into a conical flask containing 250 mL of 20% (by volume) solution of concentrated HCl in ethanol. After stirring for 18 hours, the solution was filtered over a sintered glass funnel on a Buchner flask connected to a water aspirator, and analysed by GC.

Approaches towards the synthesis of bulky analogues [ArNC(Ind)]$_2$, Ar = 2,6- $Me_2C_6H_3$, (5) and 2,6- $iPr_2C_6H_3$, (6)

A pale yellow solution of lithium indenide (1.470g, 12 mmol) in Et_2O (30 mL) was added dropwise to a yellow solution of precursor [ArNC(Cl)]$_2$, Ar = 2,6- $Me_2C_6H_3$ (2.005g, 6 mmol) in Et_2O (50 mL) at -78 ºC. The reaction mixture was allowed to return to room temperature under stirring, giving a deep orange suspension after 17 hours which turns dark

orangy-green after a further 60 hours. Removal of volatiles, washing with Et_20 (20 m1) followed by pentane (20m1) affords a bright orange solution and a brown-green solid. Filtration and removal of the solvent *in vacuo* gives a bright orange solid, **5**. (Yield: 1.129 g). Toluene (20 mL) was added to the remaining solid, yielding small amounts of a green-brown insoluble solid and a dark orange solution. Removal of the solvent *in vacuo* gives 0.362g of dark orange solid whose ^{1}H NMR spectrum (CD-2C12) shows it to be a mixture of starting materials and the desired product (**5**) as a mixture of isomers.

The preparation of the diisopropyl analogue, **6**, was attempted via a similar method using excess lithium indenide (0.465g, 38 mmol) and the $[ArNC(Cl)]_2$, Ar = 2,6- $iPr_2C_6H_3$ diimine (0.800g, 18 mmol) using THF as the solvent. After 60 hours of stirring, a dark green solution was obtained which yielded a solid of the same colour on removal of the solvent. Upon washing with pentane (20 mL), filtration and removal of solvent yields yellow oil (shown by the ^{1}H NMR spectrum to be unreacted [ArNC(Cl)] starting material). Washing the remaining solid fraction with toluene (20 mL) afforded a green solution and some insoluble solid. The mixture was filtered, and solvent removed *in vacuo* to give a green solid (0.273g) which was identified by NMR as the desired compound 6, as a mixture of isomers.

Two Photon Fluorescence spectroscopy

The solution measurements of **1** and **2** were carried out in DMSO solutions with concentration of 10 mM. Fluorescence emission lifetime components data were processed using SPCImage analysis software (Becker and Hickl, Germany) or Edinburgh Instruments F900 TCSPC analysis software. The data profile includes the goodness of fit of the decay curves as χ^2, and the lifetime of each component and their weighting of each component are given in Table 2. The χ^2 value of ca 1.0 means an optimal single exponential fit of this measurement. If the χ^2 value is more than 1.3 there is an incomplete single exponential fit of this measurement, and this was the case here. High χ^2 values (>1.5) mean either significant noise within the TCSPC setup (electronics and/or excitation source) or more than one component decay profile. Here, for both Compounds 1 and 2 fluorescence lifetimes were found to decay as two component systems, with minor components (τ_2) in the order of several nanoseconds and major components (τ_1) in the order of several hundred picoseconds (Table 3). The TSPC spectrum of **2** displays a similar decay behavior to that of **1** and in both cases evidence of some aggregation (in line with the X-ray structural observations, Figures 2 and 4) may account for the extremely short lifetime components present in the decays spectra and the χ^2 of 1.43 and 1.49 respectively, in indicating a reasonable fit for this multi-exponential model which also accounts for the aggregation features, consistent with the crystallography observations, regarding possibility of aromatic stacking in the solid state as well as the possibility of H-bonding interactions in solution with DMSO.

Table 3. Lifetime decay constants for compounds **1** and **2** point decay recorded in pure DMSO solutions (10 mM)

Compounds	τ_1 / ns	A_1 %	τ_2 / ns	A_2 %	χ^2
1	0.3	87	2.0	13	1.43
2	0.3	63	3.5	37	1.49

CONCLUSIONS

We report here our attempts to synthesize a new family of bis(indene) substituted alpha-diimines of the type $[(C_9H_7)C=N\text{-aryl}]_2$, from the reaction of chlorine substituted alpha-diimines, $(ClC=N\text{-aryl})_2$, with 2 equiv. of lithium indenyl. The ultimate goal was the use of $[(C_9H_7)C=N\text{-aryl}]_2$ as ligand precursors to heterobimetallic complexes containing in the same molecule two moieties: (a) a Zr ansa-metallocene part, and, (b) an alpha-diimine ligand coordinated to a group10 metal (Ni, Pd, Pt) counterpart; upon activation, this bimetallic system could work as catalyst for olefin oligomerisation and polymerisation or copolymerization.

However, the chemistry revealed to be quite complex since dienamine tautomers $[(C_9H_6)C\text{-}N(H)\text{-aryl}]_2$ (aryl=C_6H_5 (**1**), 2,6-$R_2C_6H_3$; R=Me (**5**), iPr (**6**)) were obtained instead of the desired $[(C_9H_7)C=N\text{-aryl}]_2$. In fact, the reactions of the dienamine tautomers (where aryl= C_6H_5) with metal compounds, such as $[Zr(NMe_2)_4]$, $[NiBr_2(DME)]$, $[PdCl_2(PhCN)_2]$ or $[PtMe_2(COD)]$, gave rise either to uncharacterised products (Zr), rather complicated mixtures of metal complexes (Ni and Pd) or a fluorescent pi-extended ring fused organic diamine resulting from an intramolecular ring coupling of the two indenyl fragments in compound **1** (Pt).

We were fascinated by the fact that the reaction between lithium indenyl and chlorine substituted alpha diimides of the form $[\{Cl(NR)_2\}C)]_2$ (R = Ph, 2,6-MeC_6H_3, 2,6-$iPrC_6H_3$) yielded serendipitously the corresponding di-enamines as the C-N(H) rearranged derivatives quantitatively, rather than the expected symmetrical alpha-diimines and proceeded to investigate the spectroscopic properties of the resulting compound and its reactivity. The enamine form, **B** of compound $[PhN(H)C(Ind)]_2$ was found to be the most kinetically favoured compound. Such products were characterised by NMR and mass spectrometry, and, in case of R=Ph, additionally by X-ray diffraction. The compound **1** was further reacted with the organometallic and coordination compound precursors incorporating transition metals such as Ni(II) and Pd(II) precursors, which gave rise to new complexes featuring both the enamine and imine bonding motifs. Interestingly, compound **1,** as well as its coupled reaction product **2**, both show some interesting fluorescence emission properties in wet DMSO conditions, and their fluorescence emission lifetimes were determined.

In summary, a new and highly conjugated flat aromatic derivative with two 5-carbon rings fused in an alternating manner with three 6-carbon member rings, **2**, has been synthesised and structurally characterised both in the solid state and in solution. NMR spectroscopy, as well as 2-photon fluorescence spectroscopy in solution, provided further evidence for the function and structural forms of **1** and of the corresponding coupled derivative **2**. Single crystal X-ray diffraction studies confirm that **2** is a new flat aromatic organic compound which features coupled indenyl residues and delocalised C-C bonds in the solid state. This strategy set out initially to give new heterobimetallic compounds leads to new organic aromatics on a facile and clean lab scale procedure, with potential fluorescence emissive potentials.

APPENDIX A. SUPPLEMENTARY DATA

CCDC 1474229 contains the supplementary crystallographic data for compound **1B** and CCDC 1474223 contains the supplementary crystallographic data for compound **2**. These data can be obtained free of charge via http://www.ccdc.cam.ac.uk/conts/retrieving.html, or from the Cambridge Crystallographic Data Centre, 12 Union Road, Cambridge CB2 1EZ, UK; fax: (+44) 1223-336-033; or e-mail: deposit@ccdc.cam.ac.uk.

ACKNOWLEDGEMENTS

SIP thanks the ERC Consolidator grant 'O2Sense' for funding and Balliol College Oxford for a Dervorguilla Scholarship, also the Royal Society for funding and the EPSRC Natonal Mass spectrometry service at Swansea as well as Colin Sparrow (Oxford) for mass spectrometry support. CTChen would like to thank the Ministry of Science and Technology of the Republic of China for financial support (grant number MOST 104-2113-M-005-014).

References

[1] L.K. Johnson, C.M. Killian, M. Brookhart, New Pd(II)- and Ni(II)-Based Catalysts for Polymerization of Ethylene and .alpha.-Olefins, Journal of the American Chemical Society, 117 (1995) 6414-6415.
[2] M. Brookhart, D.M. Lincoln, Comparison of migratory aptitudes of hydride and alkyl groups in .beta.-migratory insertion reactions of Cp*(P(OMe)3)Rh(C2H4)R+ (R = H, CH2CH3), Journal of the American Chemical Society, 110 (1988) 8719-8720.
[3] M. Brookhart, F.C. Rix, J.M. DeSimone, J.C. Barborak, Palladium(II) catalysts for living alternating copolymerization of olefins and carbon monoxide, Journal of the American Chemical Society, 114 (1992) 5894-5895.
[4] M. Brookhart, A.F. Volpe, D.M. Lincoln, I.T. Horvath, J.M. Millar, Detection of an alkyl ethylene complex during ethylene polymerization by a cobalt(III) catalyst. Energetics of the .beta.-migratory insertion reaction, Journal of the American Chemical Society, 112 (1990) 5634-5636.
[5] C.M. Killian, D.J. Tempel, L.K. Johnson, M. Brookhart, Living Polymerization of α-Olefins Using NiII−α-Diimine Catalysts. Synthesis of New Block Polymers Based on α-Olefins, Journal of the American Chemical Society, 118 (1996) 11664-11665.
[6] G.V. Koten, K. Vrieze, 1,4-Diaza-1,3-butadiene (α-Diimine) Ligands: Their Coordination Modes and the Reactivity of Their Metal Complexes, in: F.G.A. Stone, W. Robert (Eds.) Advances in Organometallic Chemistry, Academic Press, 1982, pp. 151-239.
[7] B.P. Carrow, K. Nozaki, Transition-Metal-Catalyzed Functional Polyolefin Synthesis: Effecting Control through Chelating Ancillary Ligand Design and Mechanistic Insights, Macromolecules (Washington, DC, U. S.), 47 (2014) 2541-2555.
[8] S.I. Pascu, G. Balazs, J.C. Green, M.L.H. Green, I.C. Vei, J.E. Warren, C. Windsor, Synthesis and structural investigations of Ni(II)- and Pd(II)-coordinated α-diimines with chlorinated backbones, Inorganica Chimica Acta, 363 (2010) 1157-1172.
[9] G.M. Diamond, R.F. Jordan, J.L. Petersen, Synthesis, Structure, and Reactivity of rac-Me2Si(indenyl)2Zr(NMe2)2, Organometallics, 15 (1996) 4038-4044.
[10] J.G. Stark, H.G. Wallace, Chemistry Data Book, 1982.
[11] R. van Asselt, C.J. Elsevier, W.J.J. Smeets, A.L. Spek, R. Benedix, Synthesis and characterization of rigid bidentate nitrogen ligands and some examples of coordination to divalent palladium. X-ray crystal structures of bis (p-tolylimino) acenaphthene and methylchloro [bis(o,o′-diisopropylphenyl-imino) acenaphthene] palladium (II), Recueil des Travaux Chimiques des Pays-Bas, 113 (1994) 88-98.
[12] D.P. Gates, S.A. Svejda, E. Oñate, C.M. Killian, L.K. Johnson, P.S. White, M. Brookhart, Synthesis of Branched Polyethylene Using (α-Diimine)nickel(II) Catalysts: Influence of Temperature, Ethylene Pressure, and Ligand Structure on Polymer Properties, Macromolecules, 33 (2000) 2320-2334.
[13] G. Buehrdel, R. Beckert, H. Goerls, Fulvadienes derived from fluorenes and their oxidation to spirodiazatetracenes, Synthesis, (2010) 2049-2056.
[14] C.H. Lee, Y.-H. La, J.W. Park, Zirconium(IV) Complexes Having a Rigid 1,8-Naphthalene Diamide versus a Flexible 1,3-Propylene Diamide for Olefin Polymerization, Organometallics, 19 (2000) 344-351.
[15] S.A. Svejda, M. Brookhart, Ethylene Oligomerization and Propylene Dimerization Using Cationic (α-Diimine)nickel(II) Catalysts, Organometallics, 18 (1999) 65-74.
[16] B. Zhao, K.R. Squire, S. Kacker, J.A.M. Canich, Soluble Group 10 alpha-diimine catalyst precursors, catalysts and dimerizing and oligomerizing olefins, in, Exxonmobil Chemical Patents Inc., USA . 2004, pp. 31 pp.
[17] J.M. Rose, F. Deplace, N.A. Lynd, Z. Wang, A. Hotta, E.B. Lobkovsky, E.J. Kramer, G.W. Coates, C2-Symmetric Ni(II) α-Diimines Featuring Cumyl-Derived Ligands: Synthesis of Improved Elastomeric Regioblock Polypropylenes, Macromolecules (Washington, DC, U. S.), 41 (2008) 9548-9555.
[18] R.K. O'Reilly, M.P. Shaver, V.C. Gibson, A.J.P. White, α-Diimine, Diamine, and Diphosphine Iron Catalysts for the Controlled Radical Polymerization of Styrene and Acrylate Monomers, Macromolecules (Washington, DC, U. S.), 40 (2007) 7441-7452.
[19] G. Jin, D. Zhang, Polymeric "cyclopentadienyl" α-diimino Ni-based catalyst for olefin polymerization, in, Chinese Academy of Sciences, Changchun Institute of Applied Chemistry, Peop. Rep. China . 2002, pp. 19 pp.
[20] B.K. Long, J.M. Eagan, M. Mulzer, G.W. Coates, Semi-Crystalline Polar Polyethylene: Ester-Functionalized Linear Polyolefins Enabled by a Functional-Group-Tolerant, Cationic Nickel Catalyst, Angew. Chem., Int. Ed., 55 (2016) 7106-7110.
[21] I. Matos, S.N. Fernandes, H.-R. Liu, A.K. Tevtia, R.P. Singh, M. Lemos, F. Lemos, M.M. Marques, Copolymerization of ethylene with unsaturated alcohols and methyl methacrylate using a silylated α-diimine nickel catalyst: Molecular modeling and photodegradation studies, J. Appl. Polym. Sci., 129 (2013) 1820-1832.
[22] A.S. Ionkin, W.J. Marshall, ortho-5-Methylfuran- and Benzofuran-Substituted η3-Allyl(α-diimine)nickel(II) Complexes: Syntheses, Structural Characterization, and the First Polymerization Results, Organometallics, 23 (2004) 3276-3283.

[23] D.D.S. Martini, R.F.D. Souza, S.M.P. Meneghetti, R.S. Mauler, M.J.R. Cavalcanti, Process for production of polyolefins by ethylene polymn. at high pressure and temperature using Ni-α-diimine catalysts, in, Politeno Industria E Comercio S/A, Brazil . 2007, pp. 34pp.
[24] R.J. Hue, M.P. Cibuzar, I.A. Tonks, Analysis of Polymeryl Chain Transfer Between Group 10 Metals and Main Group Alkyls during Ethylene Polymerization, ACS Catal., 4 (2014) 4223-4231.
[25] M.S. Brookhart, L.K. Johnson, C.M. Killian, E.F. McCord, S.J. McLain, K.A. Kreutzer, S.D. Ittel, D.J. Tempel, Highly branched olefin polymers and their uses, in, E. I. Du Pont de Nemours & Co., USA . 1999, pp. 122 pp., Cont.-in-part of U.S. Ser. No. 473,590, abandoned.
[26] N.W. Eilerts, B. Hauger, M.B. Welch, H.R. Deck, A dual catalyst system and polymerization process for manufacture of polyolefins with multimodal molecular weight distribution, in, Phillips Petroleum Co., USA . 2001, pp. 8 pp.
[27] M. Gasperini, F. Ragaini, S. Cenini, Synthesis of Ar-BIAN Ligands (Ar-BIAN = Bis(aryl)acenaphthenequinonediimine) Having Strong Electron-Withdrawing Substituents on the Aryl Rings and Their Relative Coordination Strength toward Palladium(0) and -(II) Complexes, Organometallics, 21 (2002) 2950-2957.
[28] P. Huo, W. Liu, X. He, Z. Wei, Y. Chen, Substituent effects and activation mechanism of norbornene polymerization catalyzed by three-dimensional geometry α-diimine palladium complexes, Polym. Chem., 5 (2014) 1210-1218.
[29] T. Dohler, H. Gorls, D. Walther, Di- and oligo-nuclear nickel complexes with oxalic amidinato bridging ligands: syntheses, structures and catalytic reactions, Chemical Communications, (2000) 945-946.
[30] C. Bianchini, A. Meli, Alternating copolymerization of carbon monoxide and olefins by single-site metal catalysis, Coordination Chemistry Reviews, 225 (2002) 35-66.
[31] P. Huo, W. Liu, X. He, H. Wang, Y. Chen, Nickel(II) Complexes with Three-Dimensional Geometry α-Diimine Ligands: Synthesis and Catalytic Activity toward Copolymerization of Norbornene, Organometallics, 32 (2013) 2291-2299.
[32] C.R. Goldsmith, F. Bronston, C. Koellner, N.A. Piro, W.S. Kassel, C.R. Graves, Group 13 metal-containing catalysts and the development of more sustainable hydrocarbon oxidation reactions, in, American Chemical Society, 2015, pp. INOR-106.
[33] C. Carfagna, G. Gatti, P. Paoli, B. Binotti, F. Fini, A. Passeri, P. Rossi, B. Gabriele, New Aryl α-Diimine Palladium(II) Catalysts in Stereocontrolled CO/Vinyl Arene Copolymerization, Organometallics, 33 (2014) 129-144.
[34] C. Redshaw, M. Walton, L. Clowes, D.L. Hughes, A.-M. Fuller, Y. Chao, A. Walton, V. Sumerin, P. Elo, I. Soshnikov, W. Zhao, W.-H. Sun, Highly Active, Thermally Stable, Ethylene-Polymerisation Pre-Catalysts Based on Niobium/Tantalum-imine Systems, Chem. - Eur. J., 19 (2013) 8884-8899.
[35] T. Shribman, S. Kurz, U. Senff, F. Lindberg, E. Hey-Hawkins, M.S. Eisen, Catalytic polymerization of propylene by heterobimetallic bridged early/late transition metal complexes, J. Mol. Catal. A: Chem., 129 (1998) 191-198.
[36] M. Tanabiki, K. Tsuchiya, Y. Motoyama, H. Nagashima, Monometallic and heterobimetallic azanickellacycles as ethylene polymerization catalysts, Chem Commun (Camb), (2005) 3409-3411.
[37] J. Kuwabara, D. Takeuchi, K. Osakada, Early-late heterobimetallic complexes as initiator for ethylene polymerization. Cooperative effect of two metal centers to afford highly branched polyethylene, Chem. Commun. (Cambridge, U. K.), (2006) 3815-3817.
[38] H.-C. Chiu, I.A. Tonks, Synthesis, reactivity, and catalystic behavior of heterobimetallic cooperative complexes based on a β-oxo-δ-diiminate ligand, in, American Chemical Society, 2015, pp. INOR-881.
[39] C. Bianchini, G. Giambastiani, A. Toti, Early-late heterobimetallic complexes as initiators for ethylene polymerization: cooperative effect of two metal centers to afford highly branched polyethylene, Chemtracts, 20 (2007) 107-111.
[40] S.V. Kulangara, A. Jabri, Y. Yang, I. Korobkov, S. Gambarotta, R. Duchateau, Synthesis, X-ray Structural Analysis, and Ethylene Polymerization Studies of Group IV Metal Heterobimetallic Aluminum-Pyrrolyl Complexes, Organometallics, 31 (2012) 6085-6094.
[41] E. Petrlikova, K. Waisser, G. Buhrdel, R. Beckert, J. Kaustova, Search for new antituberculotics, Folia Pharm. Univ. Carol., 38 (2010) 15-17.
[42] R. Figueroa, R.D. Froese, Y. He, J. Klosin, C.N. Theriault, K.A. Abboud, Synthesis of imino-enamido hafnium and zirconium complexes: A new family of olefin polymerization catalysts with ultrahigh-molecular-weight capabilities, Organometallics, 30 (2011) 1695-1709.
[43] S. Collins, R.A. Stapleton, J. Chai, A. Nuamthanom, P.L. Rinaldi, J.B.P. Soares, Z. Flisak, T. Ziegler, Synthesis of low density polyethylene using Ni iminophosphonamide catalysts, in, American Chemical Society, 2006, pp. INOR-547.
[44] C. Fritze, G. Erker, R. Fröhlich, Formation of tetrabenzodispiro[4.0.4.3]tridecatetraene by a titanium mediated fluorenyl coupling reaction, Journal of Organometallic Chemistry, 501 (1995) 41-45.
[45] G. Wilkinson, R.D. Gillard, J.A. McCleverty, Compreshensive Coordination Chemistry. The Synthesis, Reactions, Properties and Applications of Coordination Compounds, Pergamon Press, 1987.
[46] G. Wilkinson, F.G.A. Stone, E.W. Abel, Comprehensive Organometallic Chemistry II: A Review of the Literature 1982-1994 Pergamon Press, 1995.
[47] B.M. Glazier, J.A. Golen, D.R. Manke, Di-[mu]-chlorido-bis[(2,2'-bipyridine-[kappa]2N,N')chlorido(N,N-dimethylformamide-[kappa]O)nickel(II)], IUCrData, 1 (2016) x160259.
[48] M. Xie, R.E. Norman, Di-[mu]-bromo-bis[bis(1,2-diaminoethane-[kappa]2N,N)nickel(II)] dibromide, Acta Crystallographica Section E, 62 (2006) m408-m410.
[49] H.-T. Wang, Y.-Y. Song, M.Y. Chiang, W.-F. Zeng, Di-[mu]-bromo-bis{aqua[(5-bromo-1H-imidazol-4-ylmethylene)(2-pyridylmethyl)amine-[kappa]3N,N',N'']nickel(II)} dibromide, Acta Crystallographica Section E, 62 (2006) m2464-m2466.
[50] J.O. Liimatta, B. Löfgren, M. Miettinen, M. Ahlgren, M. Haukka, T.T. Pakkanen, Molecular structure determination of Ni(II) diimine complex and DMA analysis of Ni(II) diimine-based polyethenes, Journal of Polymer Science Part A: Polymer Chemistry, 39 (2001) 1426-1434.
[51] R.J. Maldanis, J.S. Wood, A. Chandrasekaran, M.D. Rausch, J.C.W. Chien, The formation and polymerization behavior of Ni(II) α-diimine complexes using various aluminum activators, Journal of Organometallic Chemistry, 645 (2002) 158-167.
[52] H.-R. Liu, P.T. Gomes, S.I. Costa, M.T. Duarte, R. Branquinho, A.C. Fernandes, J.C.W. Chien, R.P. Singh, M.M. Marques, Highly active new α-diimine nickel catalyst for the polymerization of α-olefins, Journal of Organometallic Chemistry, 690 (2005) 1314-1323.
[53] Q. Dai, X. Jia, F. Yang, C. Bai, Y. Hu, X. Zhang, Iminopyridine-Based Cobalt(II) and Nickel(II) Complexes: Synthesis, Characterization, and Their Catalytic Behaviors for 1,3-Butadiene Polymerization, Polymers, 8 (2015) 1-15.
[54] R. Caris, B.C. Peoples, M. Valderrama, G. Wu, R. Rojas, Mono and bimetallic nickel bromide complexes bearing azolate-imine ligands: Synthesis, structural characterization and ethylene polymerization studies, Journal of Organometallic Chemistry, 694 (2009) 1795-1801.
[55] W. Kaminsky, R. Engehausen, K. Zoumis, W. Spaleck, J. Rohrmann, Standardized polymerizations of ethylene and propene with bridged and unbridged metallocene derivatives: A comparison, Die Makromolekulare Chemie, 193 (1992) 1643-1651.
[56] S.D. Ittel, L.K. Johnson, M. Brookhart, Late-Metal Catalysts for Ethylene Homo- and Copolymerization, Chemical Reviews, 100 (2000) 1169-1204.
[57] G.M. Diamond, R.F. Jordan, J.L. Petersen, Efficient Synthesis of Chiral ansa-Metallocenes by Amine Elimination. Synthesis, Structure, and Reactivity of rac-(EBI)Zr(NMe2)2, Journal of the American Chemical Society, 118 (1996) 8024-8033.
[58] C.J. O'Connor, Magnetochemistry—Advances in Theory and Experimentation, in: Progress in Inorganic Chemistry, John Wiley & Sons, Inc., 2007, pp. 203-283.
[59] S.W. Botchway, A.W. Parker, R.H. Bisby, A.G. Crisostomo, Real-time cellular uptake of serotonin using fluorescence lifetime imaging with two-photon excitation, Microscopy Research and Technique, 71 (2008) 267-273.
[60] D.J. Watkin, C.K. Prout, Lilley, P.M. deQ, RC93, in, 1994.
[61] L.J. Farrugia, WINGX-v2014, , J. Appl. Crystallogr., 45 (2012) 849–854.
[62] C.F. Macrae, P.R. Edgington, P. McCabe, E. Pidcock, G.P. Shields, R. Taylor, Towler, v.d. Streek, Mercury, J. Appl. Crystallogr. , 39 (2006) 453-457.

[63] H.-J. Becher, D. Fenske, E. Langer, H. Prokscha, Structure and colour of P, P′-tetra-t-butyl-and P, P′-tetraphenyl oxalic acid diphosphide and derivatives, Monatshefte für Chemie / Chemical Monthly, 111 (1980) 749-759.
[64] T.V. Artamonova, A.B. Zhivich, M.Y. Dubinskii, G.I. Koldobskii, Preparation of 1,5-Disubstituted Tetrazoles Under Phase-Transfer Conditions, Synthesis, 1996 (1996) 1428-1430.
[65] D. Lindauer, R. Beckert, M. Döring, P. Fehling, H. Görls, Zur Aminolyse von Bis-Imidoylchloriden der Oxalsäure. I. Umsetzung mit aromatischen und aliphatischen Aminen, Journal für Praktische Chemie/Chemiker-Zeitung, 337 (1995) 143-152.

Figure 1

Click here to download high resolution image

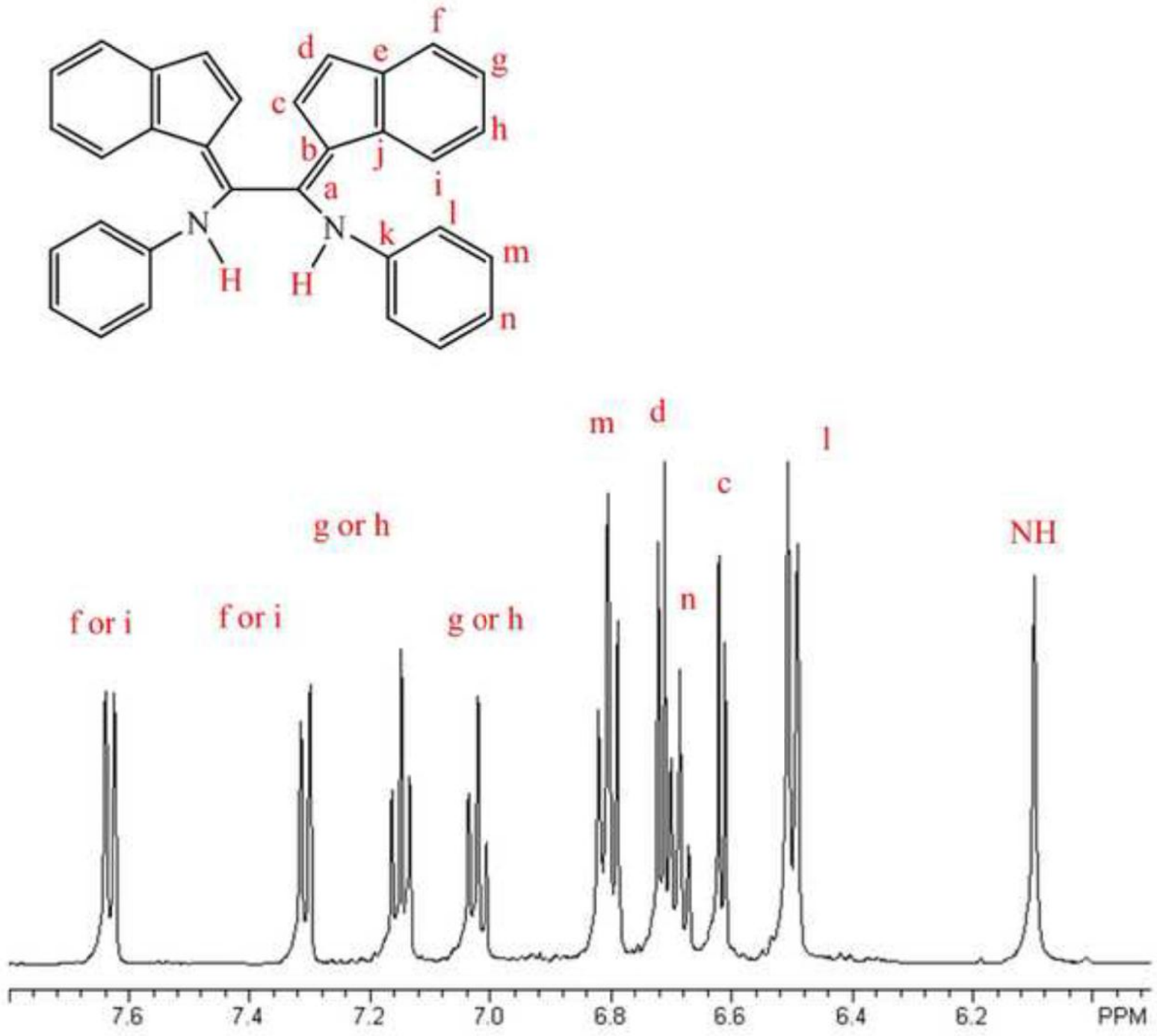

Figure 2

Click here to download high resolution image

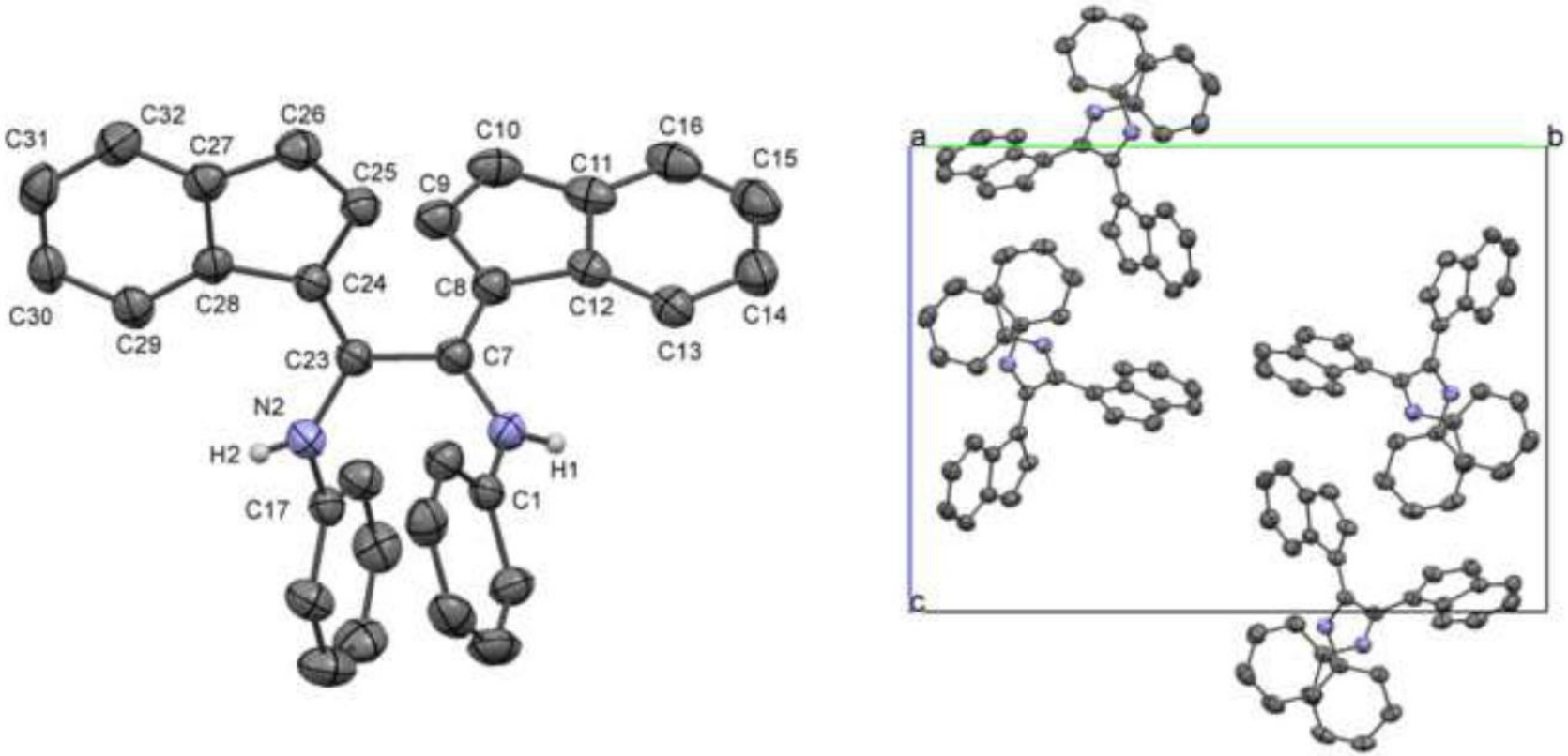

Figure 3
Click here to download high resolution image

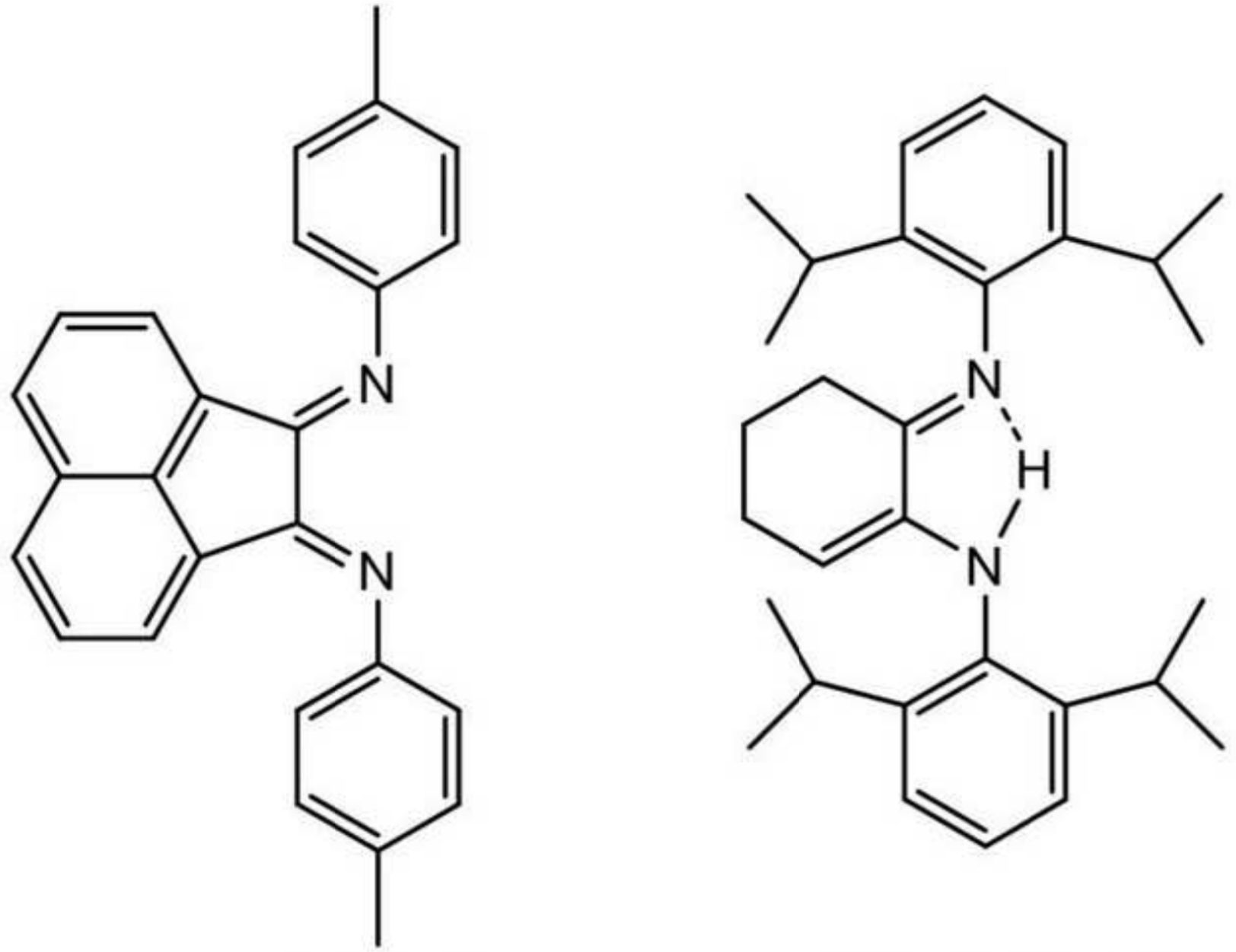

*p*Tol-BIAN

$[C_6H_3(i\text{-}Pr)_2]_2$-AIC

Figure 4

Click here to download high resolution image

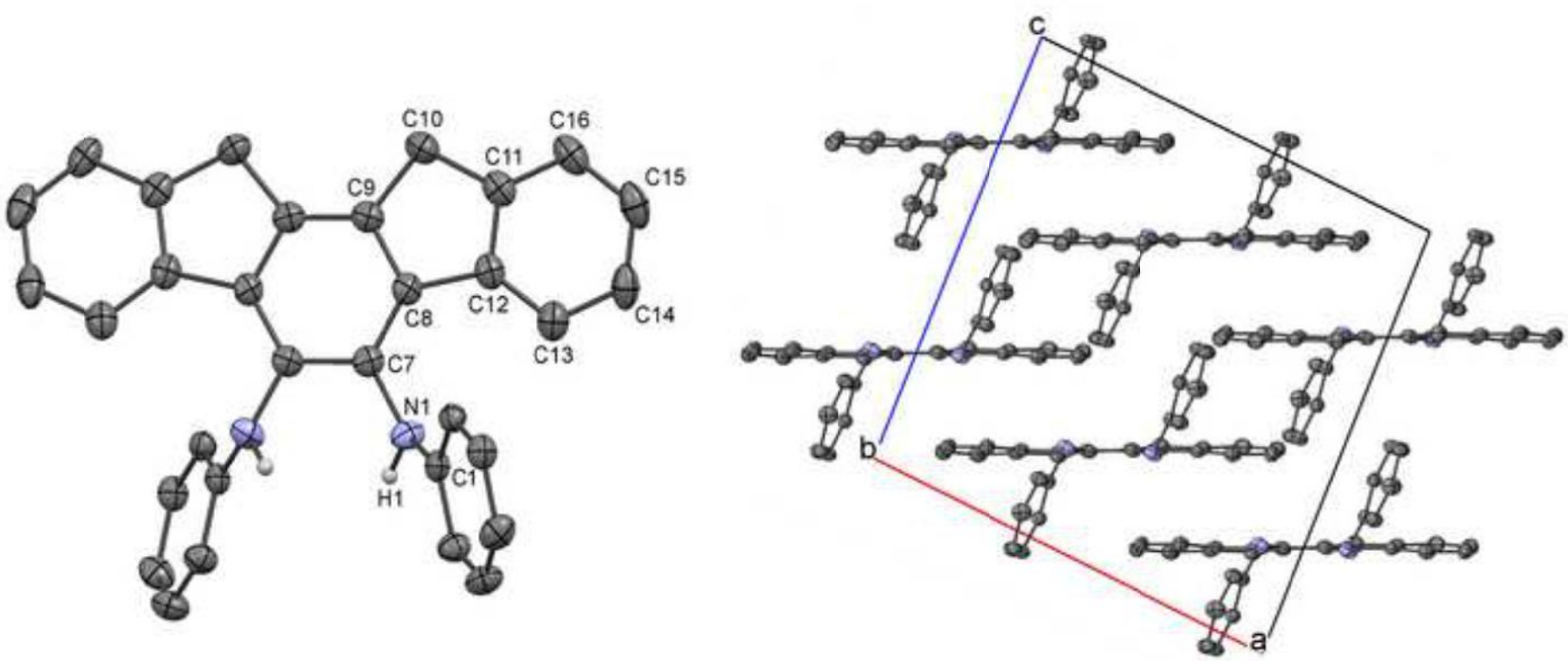

Figure 5

Click here to download high resolution image

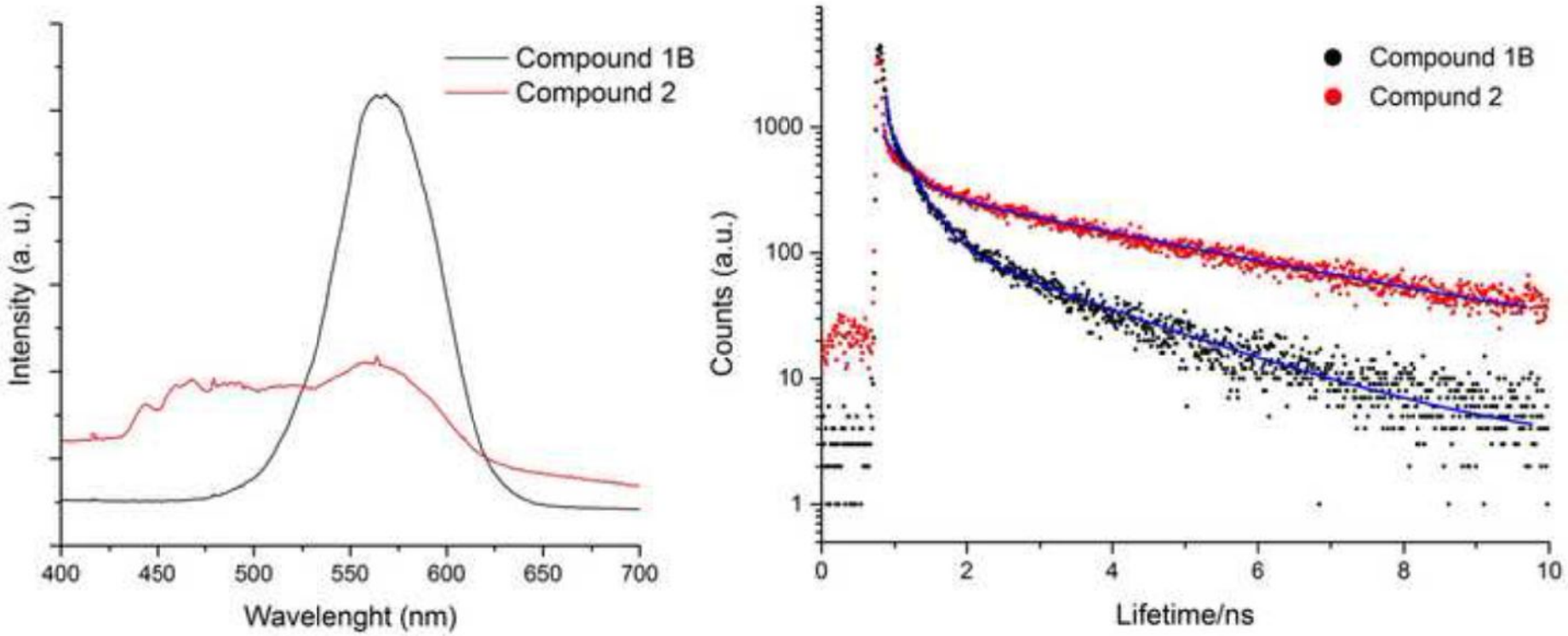

Figure 6

Click here to download high resolution image

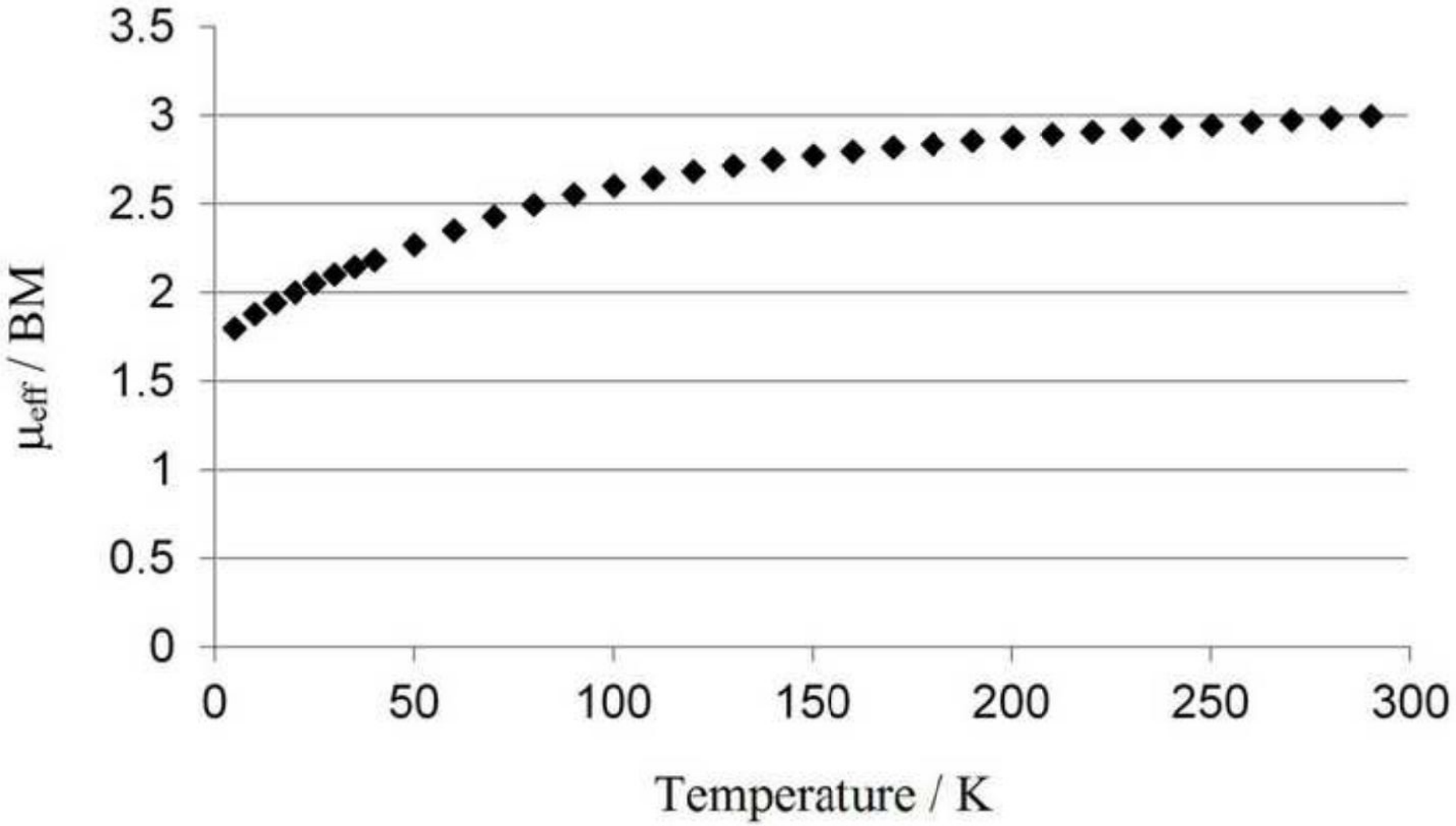

Label compound 2

Click here to download high resolution image

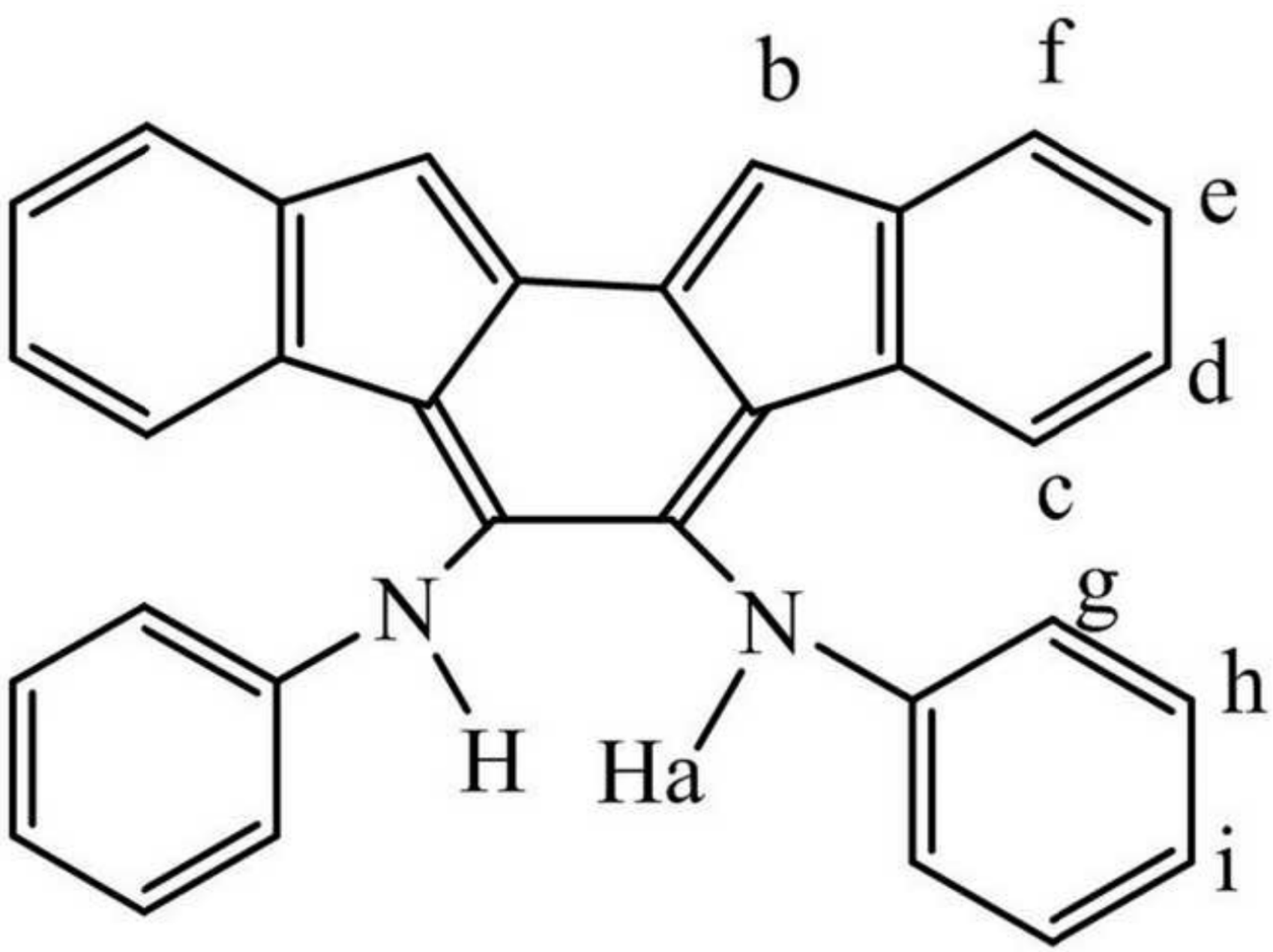

Scheme 1

Click here to download high resolution image

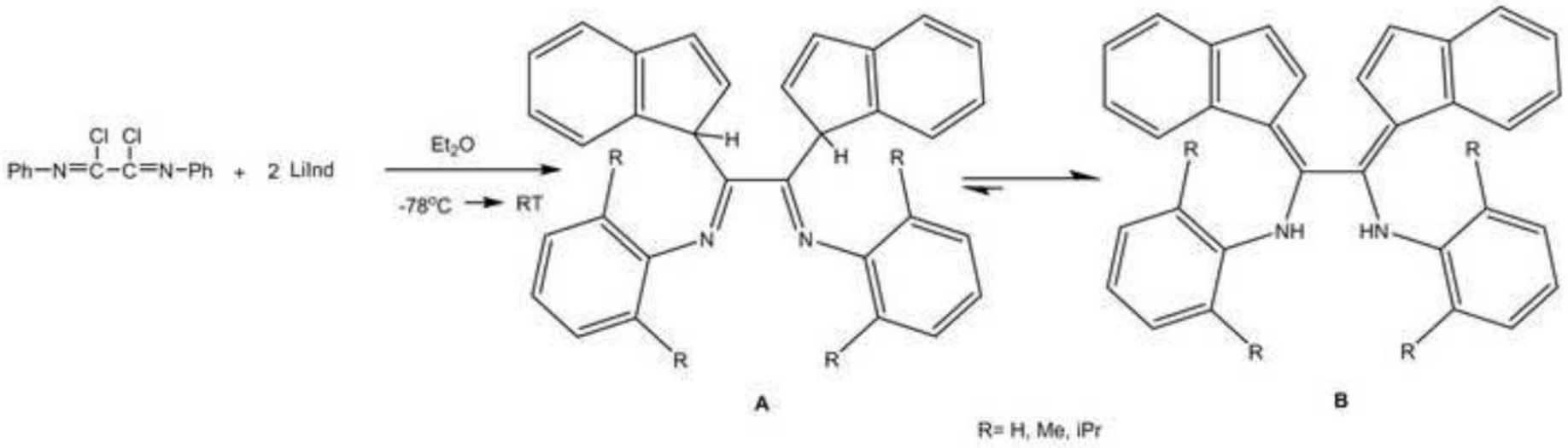

Scheme 2

Click here to download high resolution image

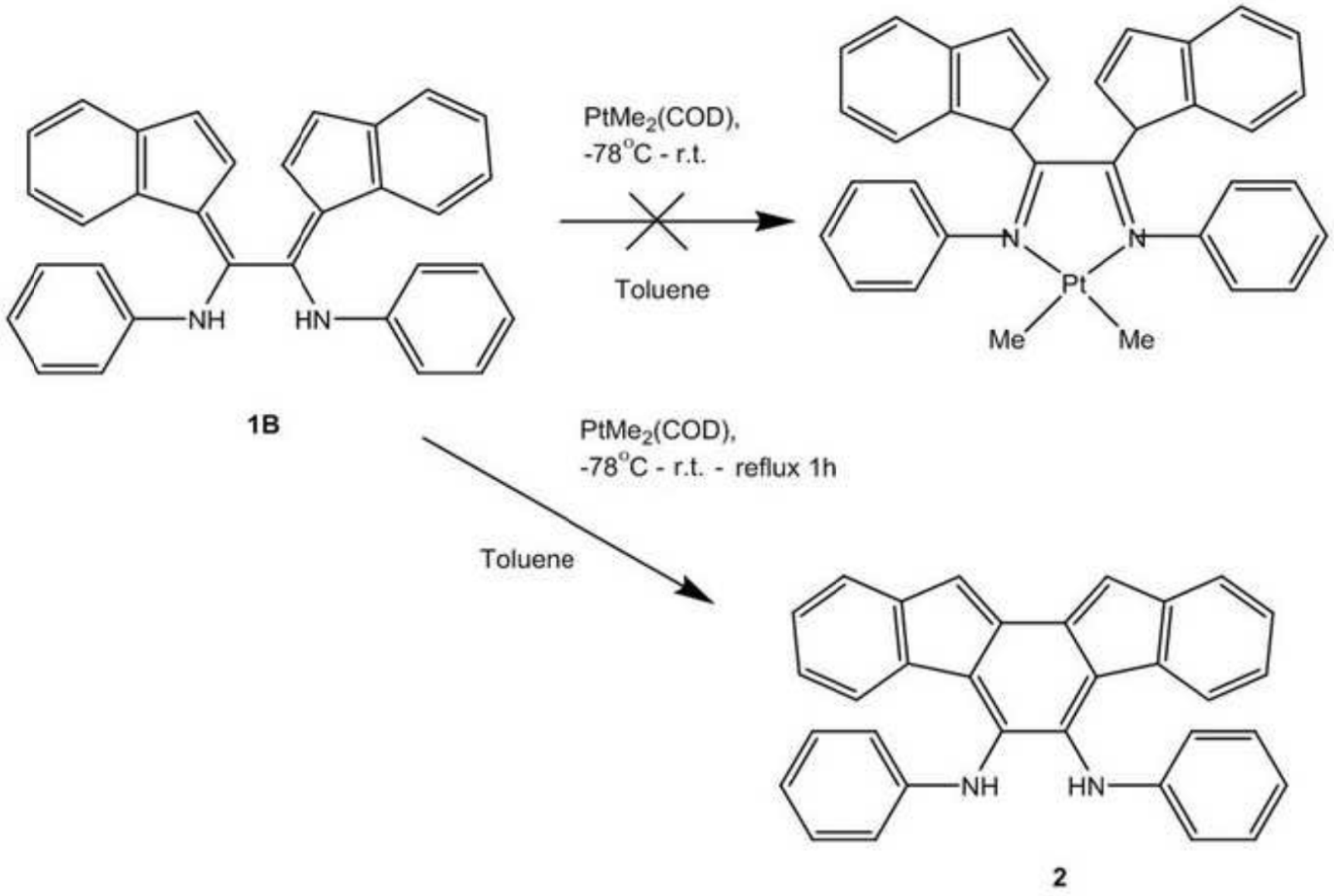

Scheme 3

Click here to download high resolution image

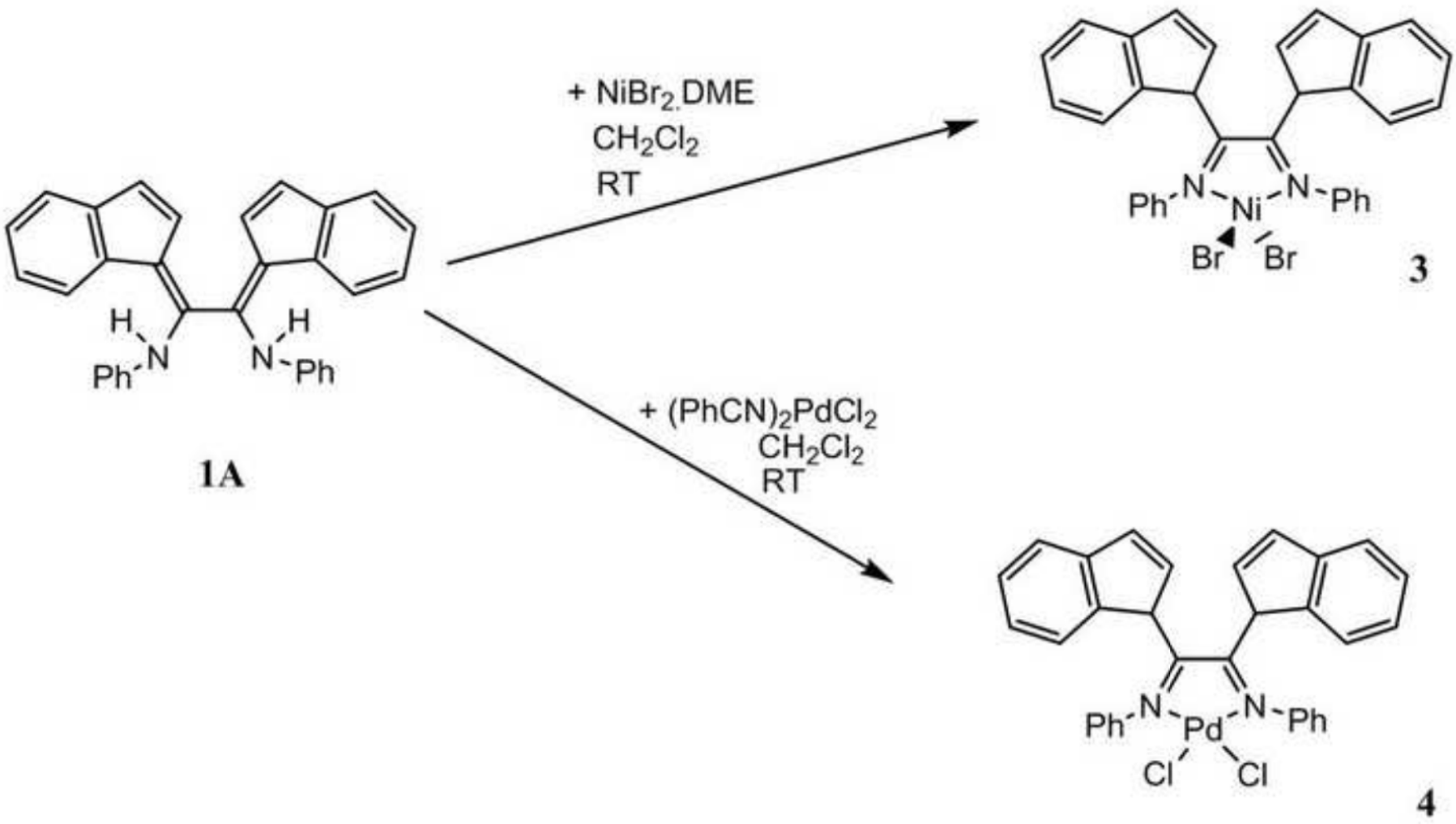

Scheme 4

Click here to download high resolution image

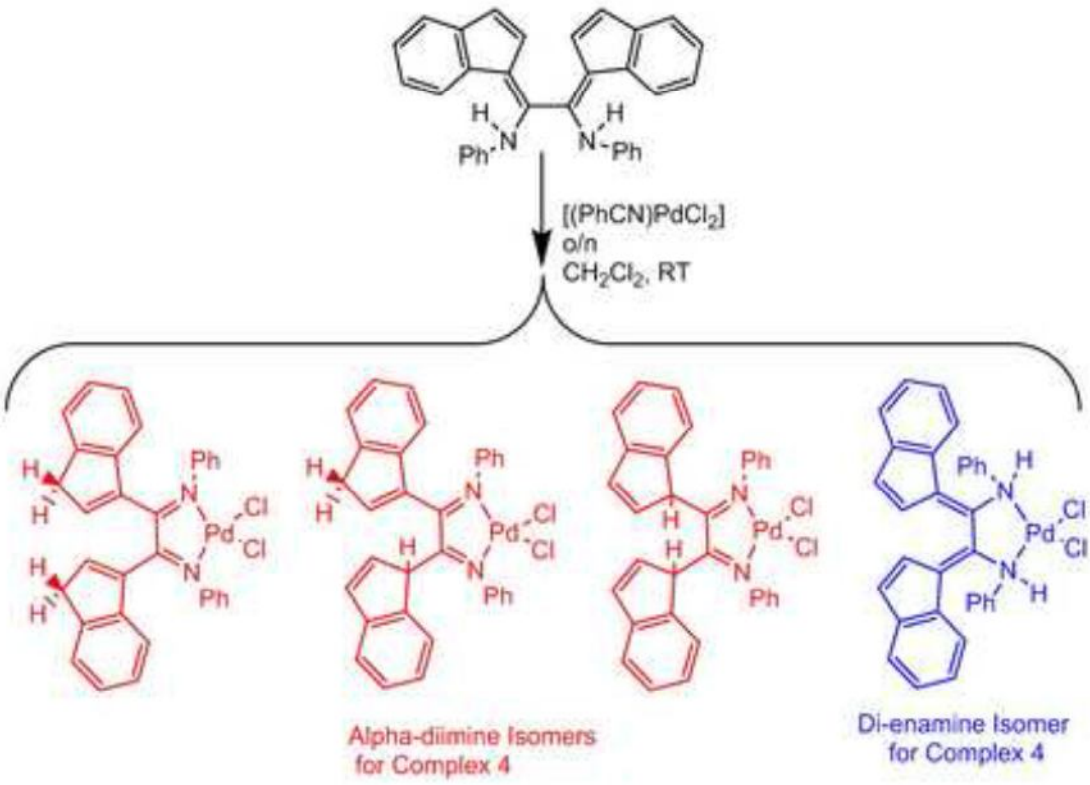

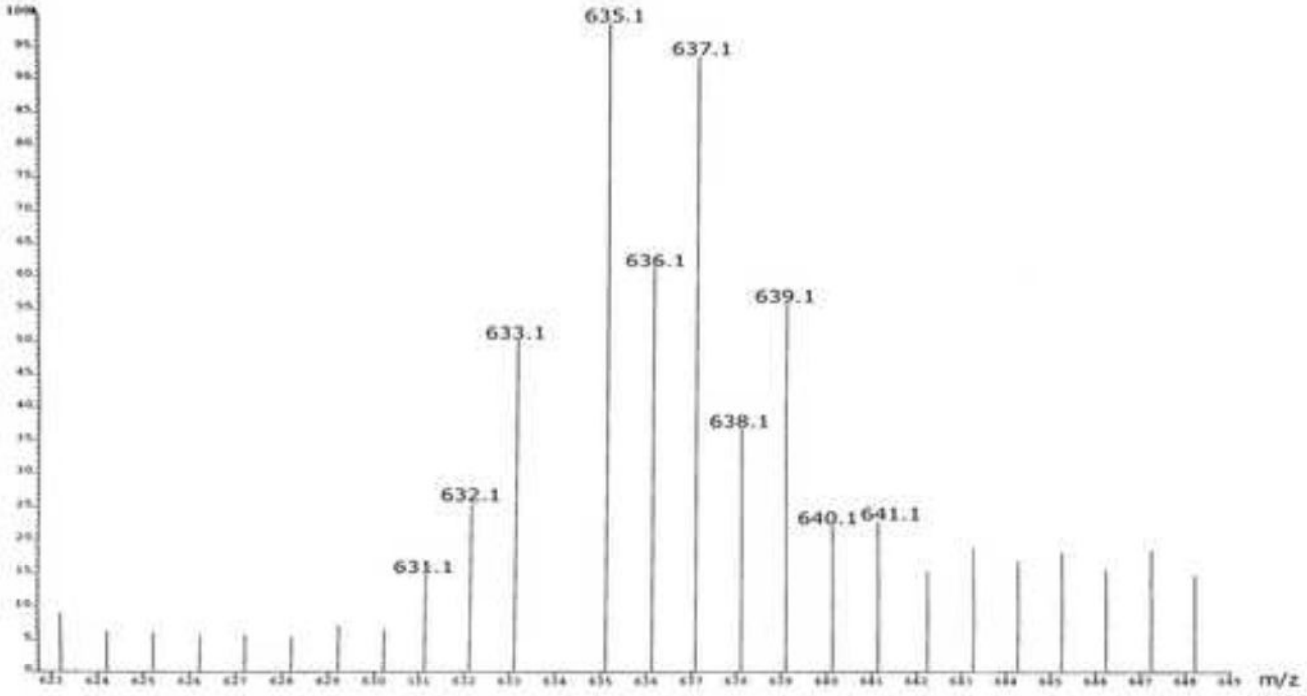

Scheme 5

Click here to download high resolution image

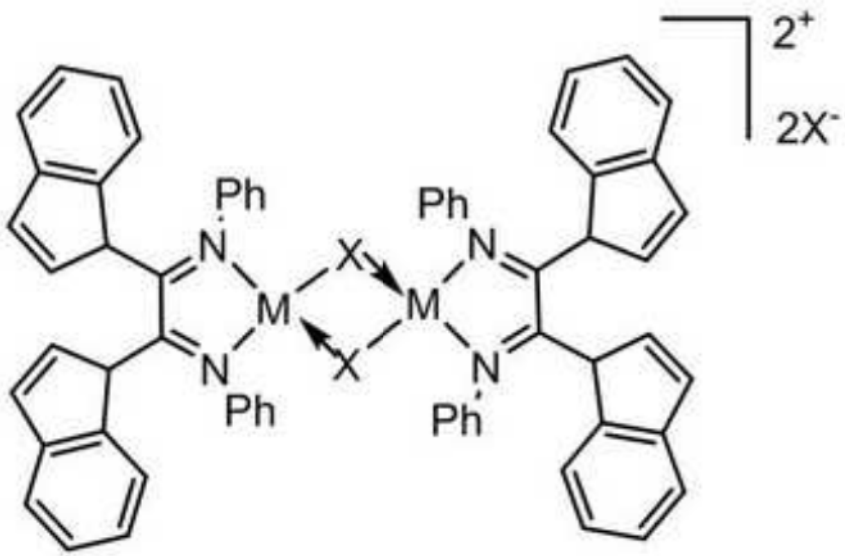

Diimine Dimer - isomer type A

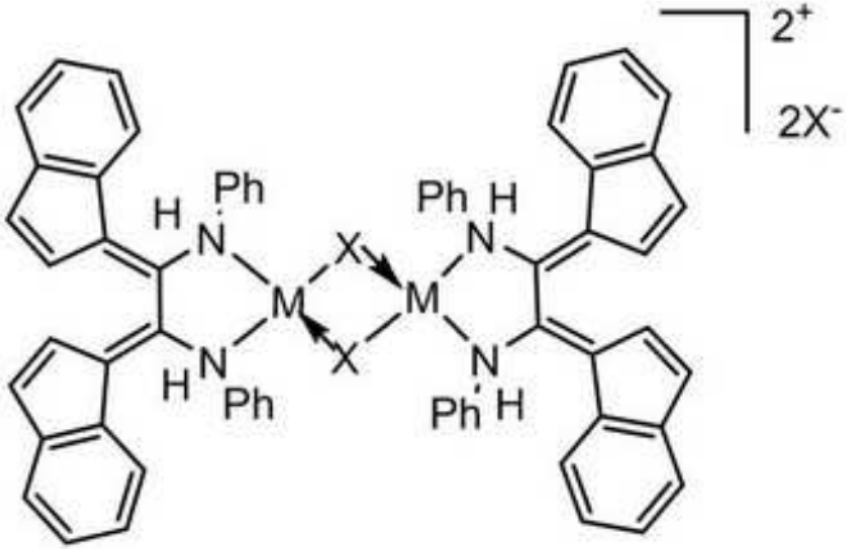

Enamine Dimer - isomer type B

M = Ni, X = Br
M=Pd, X = Cl

Scheme 6

Click here to download high resolution image

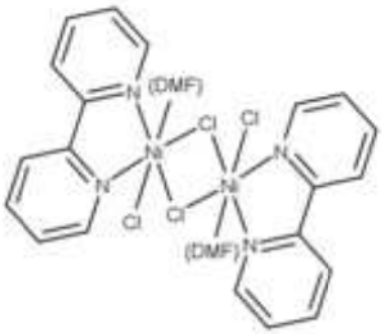

(I)

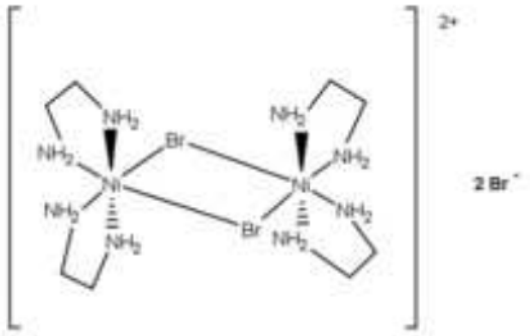

(II)

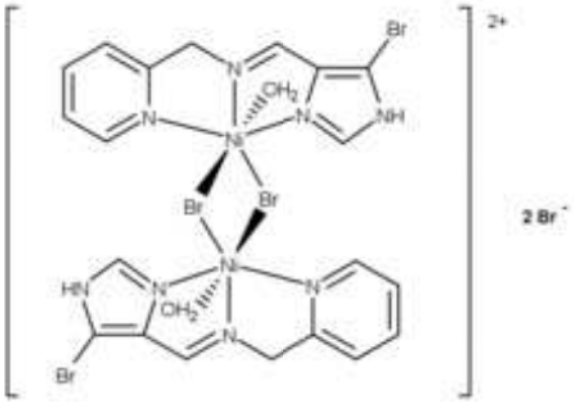

(III)

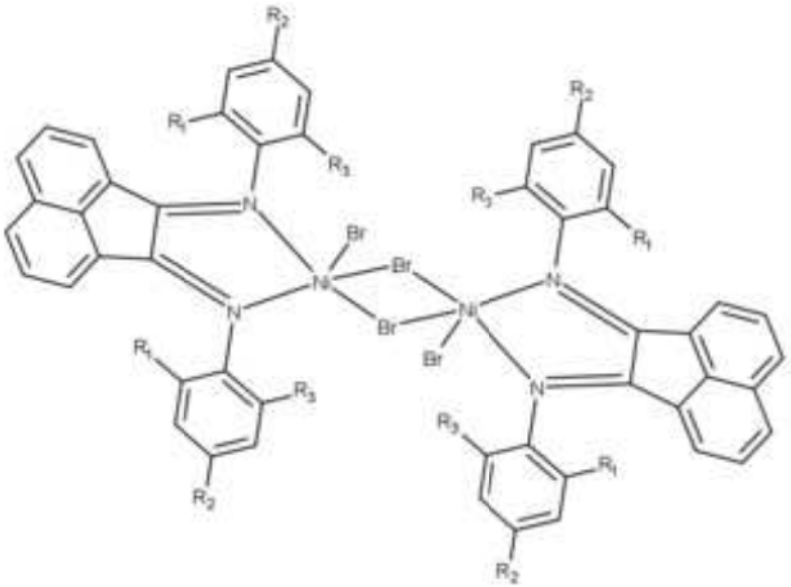

(IV) $R_{1,3}$ = ^{i}Pr; R_2 = H

(V) $R_{1,2}$ = H; R_3 = ^{t}Bu

(VI) $R_{1,3}$ = ^{i}Pr; R_2 = Si(^{t}Bu)Ph_2

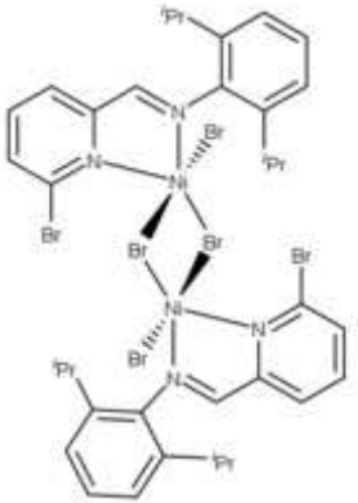

(VII)

Scheme 7

Click here to download high resolution image

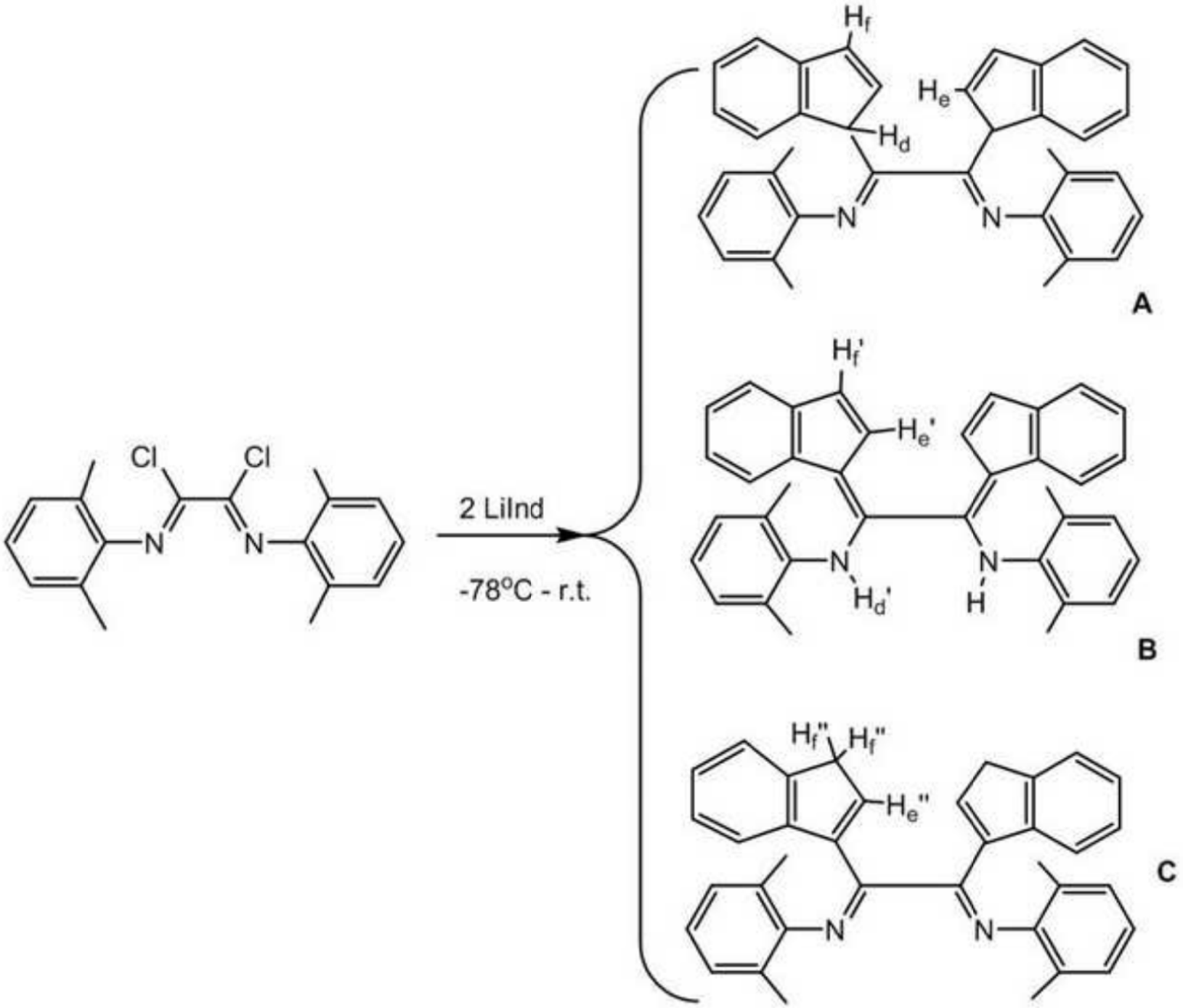

Scheme 8

Click here to download high resolution image

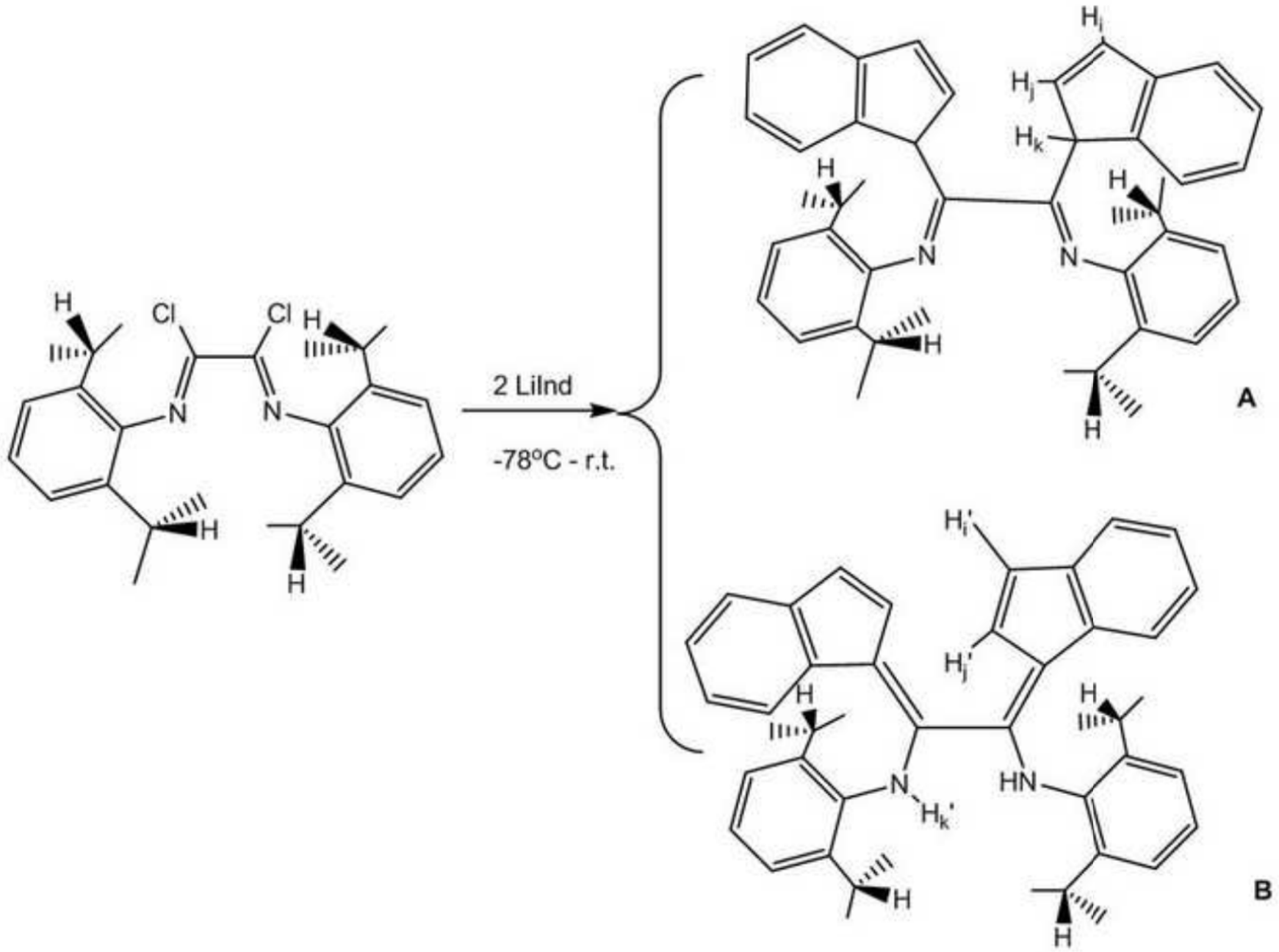

Scheme 9

Click here to download high resolution image

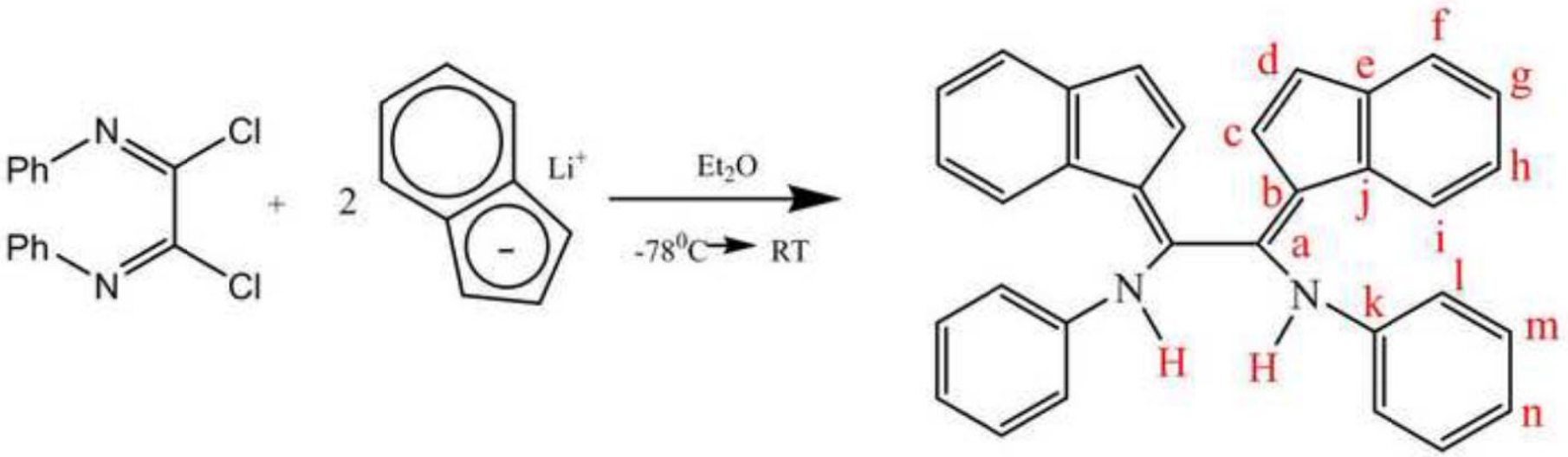

CIF (*if crystal structure is described)

Click here to download CIF (*if crystal structure is described): Publication_1B.cif

CIF (*if crystal structure is described)

Click here to download CIF (*if crystal structure is described): Publication_ 2.cif

CheckCIF (*if crystal structure is described)

Click here to download CheckCIF (*if crystal structure is described): checkcif 1B.pdf

CheckCIF (*if crystal structure is described)

Click here to download CheckCIF (*if crystal structure is described): checkcif 2.pdf

Supplementary Info for Online Publication

Click here to download Supplementary Info for Online Publication: ESI final indenyl paper SIP DGB to upload.pdf